Radiobiological Effects of Alpha-Particles from Astatine-211

From DNA Damage to Cell Death

Kristina Claesson

Department of Oncology
Institute of Clinical Sciences
The Sahlgrenska Academy at University of Gothenburg

UNIVERSITY OF
GOTHENBURG

ABSTRACT

In recent years, the use of high linear energy transfer (LET) radiation for radiotherapeutic applications has gained increased interest. Astatine-211 (^{211}At) is an α-particle emitting radionuclide, promising for targeted radioimmunotherapy of isolated tumor cells and microscopic clusters. To improve development of safe radiotherapy using ^{211}At it is important to increase our knowledge of the radiobiological effects in cells. During radiotherapy, both tumors and adjacent normal tissue will be irradiated and therefore, it is of importance to understand differences in the radioresponse between proliferating and resting cells. The aim of this thesis was to investigate effects in fibroblasts with different proliferation status after irradiation with α-particles from ^{211}At or X-rays, from inflicted DNA damage, to cellular responses and biological consequences.

Throughout this work, irradiation was performed with α-particles from ^{211}A or X-rays. The induction and repair of double-strand breaks (DSBs) in human normal fibroblasts were investigated using pulsed-field gel electrophoresis and fragment analysis. The relative biological effectiveness (RBE) of ^{211}At for DSB induction varied between 1.4 and 3.1. A small increase of DSBs was observed in cycling cells compared to stationary cells. The repair kinetics was slower after ^{211}At and more residual damage was found after 24 h. Comparison between cells with different proliferation status showed that the repair was inefficient in cycling cells with more residual damage, regardless of radiation quality. Activation of cell cycle arrests was investigated using immunofluorescent labeling of the checkpoint kinase Chk2 and by measuring cell cycle distributions with flow cytometry analysis. After α-particle irradiation, the average number of Chk2-foci was larger and the cells had a more affected cell cycle progression for several weeks compared with X-irradiated cells, indicating a more powerful arrest after ^{211}At. Flow cytometry showed that cycling cells were arrested in G$_2$/M while stationary cells underwent a delayed entry into S phase after release of contact inhibition. Radiation-induced chromosomal damage was studied by investigating the formation of micronuclei after first mitosis post-irradiation. Alpha-particles induced 2.7 and 4.1 times more micronuclei in cycling and stationary cells, respectively, compared with X-rays.

Induction of DSBs and cell survival after irradiation were also investigated in synchronized Chinese hamster fibroblasts. The cells were synchronized with mimosine in G$_1$, early, mid and late S phase and in mitosis and cell survival was determined using the clonogenic assay. The radioresponse between cell cycle phases varied after both ^{211}At and X-rays, resulting in variations of RBE for ^{211}At between 1.8 and 3.9 for DSB induction and between 3.1 and 7.9 for 37% survival. The lowest RBE was observed in mitotic cells for both DSB induction and clonogenic survival.

In summary, for all endpoints studied α-particles from ^{211}At were more detrimental compared with X-rays. Further, the radioresponse was dependent upon the proliferation status of the cells at the time of irradiation, after both low- and high-LET radiation, resulting in variations of the relative biological effects.

LIST OF PAPERS

This thesis is based on the following papers, which will be referred to in the text by their roman numerals:

I   **Claesson K,** Stenerlöw B, Jacobsson L and Elmroth K. Relative Biological Effectiveness of the α-Particle Emitter ^{211}At for Double-Strand Break Induction in Human Fibroblasts. *Radiation Research* 2007; 167, 312-318.

II   **Claesson K,** Magnander K, Kahu K, Lindegren S, Hultborn R and Elmroth K. RBE of α-Particles from ^{211}At for Complex DNA Damage and Cell Survival in Relation to Cell Cycle Position. *International Journal of Radiation Biology,* 2011; 87, 372-384.

III   **Claesson K**, Nordén Lyckesvärd M, Magnander K, Lindegren S and Elmroth K. Double-Strand Break Repair and Cell Cycle Arrest Activation in Stationary and Cycling Diploid Cells Irradiated with High- and Low-LET Radiation. *Manuscript*.

IV   **Claesson K,** Nordén Lyckesvärd M, Magnander K, Delle U and Elmroth K. Effects on Micronuclei Formation and Growth Kinetics in Normal Fibroblasts after Irradiation with Alpha Particles and X rays: Differential Response in Stationary and Cycling Cell Cultures. *Manuscript.*

TABLE OF CONTENTS

ABBREVIATIONS

Ac-H3K9	Acetylated histone 3 on lysine 9
AP	apurinic/apyrimidinic
ATM	Ataxia-telangiectasia mutated
bp	base pair
BRCA1/2	Breast cancer susceptibility protein 1/2
Chk2	Checkpoint kinase 2
DAPI	4'-6-Diamidino-2-phenylindole
DMF	Dose modifying factor
DNA	Deoxyribonucleic acid
DNA-PKcs	DNA-dependent protein kinase catalytic subunit
DSB	Double-strand break
eV	Electron voltage
FAR	Fraction of activity released
Fpg	Formamidopyrimidine-DNA glycosylase
FITC	fluorescein isothiocyanate
Gy	Gray
H2A/B, H3, H4	Histone 2A/B, Histone 3, Histone 4
H2AX	Histone 2A variant X
γ-H2AX	Phosphorylated H2AX
HDAC	Histone deacetylase inhibitor
HRR	Homologous recombination repair
LET	Linear energy transfer
LQ	Linear quadratic
MN	Micronuclei
MRE11	Meiotic recombination 11
MRN	MRE11/RAD50/NBS1 complex
NBS1	Nijmegen breakage syndrome 1
NHEJ	Non-homologous end joining
p53	Protein 53
PBS	Phosphate buffer saline
PB+	Phosphate buffer, modified
PFGE	Pulsed-field gel electrophoresis
RBE	Relative biological effectiveness
RIT	Radioimmunotherapy
SF	Surviving fraction
SSB	Single-strand break
TSA	Trichostatine A
Thr68	Threonine 68
XRCC4	X-ray repair cross complementing protein 4

INTRODUCTION

Soon after the discovery of X-rays, in 1895, by Wilhelm Konrad Roentgen and of the radioactive properties of uranium (1896) and of polonium and radium (1898) by Henry Becquerel, Marie Curie, and Pierre Curie, it become known that the biological effects in tissues after ionizing radiation could be either beneficial or noxious and the study of radiation biology was started. The breakthrough of radiobiology research on mammalian cells *in vitro* was made in the 1950s by Puck and Marcus, who developed a method for growing clones from viable cells (*1*). Today, research in radiobiology is increasingly important for our understanding of how cells and tissues are affected by ionizing radiation as a basis for future development of treatments of tumor diseases.

Today, ionizing radiation is widely used as a modality for treatment of cancer and can be used either via external radiotherapy or, internally, via radioactive nuclides. About 50% of all cancer patients in Sweden receive radiotherapy either as part of a curative or a palliative treatment. Radiation can induce irreparable damage in the cell as it ionizes atoms when the energy is transferred. As a consequence, chemical bonds in DNA, considered as the most critical target, will be broken, resulting in many types of lesions: base lesions, cross-links, apurinic/apyrimidinic (AP) sites, single-strand breaks (SSBs), and double-strand breaks (DSBs) (*2-3*). In cells, these lesions will activate a network of signaling pathways to initiate repair mechanisms and arrests in cell cycle progression, to prevent transfer of DNA lesions to the next cell generation (*4*). If not repaired correctly, signaling of cell death via apoptosis may occur, or cells may die by mitotic catastrophe during the following mitosis (*3, 5-6*).

Since DNA encodes for all cellular functions, this DNA damage response is very important in preserving the genomic integrity. However, since ionizing radiation causes damage to the genetic code also in surviving cells, there is a close correlation between exposure to ionizing radiation, and cancer induction.

Low- and High-Linear Energy Transfer Radiation

Ionizing radiation can be characterized by the density of the ionizations. The measured quantity of linear energy transfer (LET) describes the average energy transferred per unit length (keV/µm) of the track.

Low-LET radiation, e.g. X-rays, γ-rays, and electrons, is sparsely ionizing, with LET values up to a few keV/µm (3). The ionizations after the low-LET radiation track in the cell nucleus are usually well separated (2). In the case of photon radiation, the energy is transferred via secondary electrons to biomolecules (direct effect) or to the surrounding water molecules in proximity to DNA. As a result, reactive free radicals are formed from the radiolysis of water, which can damage DNA (indirect effect). It is estimated that about 70% of the damages in the DNA are caused by this indirect effect, due to high amount of water molecules, and 30% by direct action of the incident radiation on DNA (7).

High-LET radiation is densely ionizing and the LET can be up to several 100 keV/µm (3). Alpha-particles, low-energy protons, and accelerated ions are classified as high-LET radiation. In contrast to low-LET radiation, high-LET radiation deposits more energy through the direct effect of ionizing radiation (8) and transfers the energy concentrated along its track. The dose delivered by high-LET particles increases with depth and reaches its maximum at the end of the particle track, the Bragg peak, with a sharp edge and with little scatter. Such dense ionizations can cause complex DNA damage.

Relative Biological Effectiveness

To compare the biological effects in cells and tissues between different types of ionizing radiation, the definition *relative biological effectiveness* (RBE) is usually used. Relative biological effectiveness is defined as the ratio of absorbed dose (Gy) of a reference radiation quality (usually ^{60}Co and 250 keV X-rays) and the dose of a test radiation causing the same biological effect. Relative biological effectiveness is dependent on e.g. particle type, LET, absorbed dose, dose rate and number of dose fractions, as well as on the biological system and

endpoint investigated. The RBE rises with LET up to a maximum at ~100-200 keV/µm, and thereafter falls with higher LET values (*9*).

Complex DNA Damage

Double-Strand Breaks

The DNA DSB is considered to be the most biologically significant lesion (*10*). This may be due to the lack of available template for correct reconstruction of the base sequence, since both strands are damaged. A DSB is formed when the two complementary strands of the DNA double helix are broken simultaneously at sites that are sufficiently close to each other (within 10–20 bp) so that base pairing and chromatin structure are inadequate to keep the two DNA strands together (*11*). A dose of 1 Gy after low-LET irradiation induces about 20–30 DSBs/cell. With the same radiation dose of high-LET radiation, up to four times more DSBs can be induced. Double-strand breaks induced after low-LET irradiation are randomly distributed in the nucleus and usually are well separated. By contrast, irradiation with high-LET radiation generates correlated DSBs resulting in many small DNA fragments as a consequence of the dense ionizations along the particle track (*12-13*).

Clustered Damage

Clustered damages are a newly identified type of complex DNA damage. Bistranded clustered damage is defined as two or more lesions positioned on opposite strands within 10–20 bp on DNA. It can include base lesions, SSBs, AP sites, or modifications of sugars. Some of these lesions are transformed into strand breaks through enzyme activity by base excision repair systems. If these lesions are located on opposite DNA strands or close to a single-strand break, a *de novo* DSB may form (*14*). Clusters, and specifically the lesions within, are suggested to be induced predominantly by the indirect effect of radiation and depend strongly on scavenging conditions and chromatin structure (*15-17*).

DNA Damage Response

Double-Strand Break Repair

Mammalian cells are equipped with several repair systems to deal with various types of DNA lesions. There are two main pathways involved in DSB repair: non-homologous end joining (NHEJ) and homologous recombination repair (HRR), which are largely distinct from one another and function in complementary ways (*18-19*). Non-homologous end joining is the predominant repair pathway in mammalian cells, acting primarily in G_0/G_1 and early S phase, when the DNA ends are simply ligated without the need for homologous template. In addition to NHEJ and HRR, NHEJ backup and error-prone single-strand annealing are possible alternative pathways for repair of DNA damage (*20*).

The first step in NHEJ is that the heterodimer Ku70/Ku80 binds to the broken DNA ends, followed by recruitment of DNA–PKcs (*21*). The activated complex keeps the two ends together in close proximity in order for the repair process to proceed. The ends will be trimmed by the Artemis endonuclease activity which is phosphorylated by the DNA–PKcs unit (*22*). In addition to Artemis endonuclease activity, the MRE11–RAD50–NBS1 (MRN) complex may also function in NHEJ, particularly if the DNA ends require processing before ligation (*23*). The final step of NHEJ, after gaps are filled by polymerases, is that the ends will be ligated by XRCC4–DNA ligase IV (*24*).

Homologous recombination repair occurs primarily in the late S and G_2 phase, when appropriate homologous chromatid is available as a sequence template (*25*). A large number of proteins are involved in homologous recombination, including RAD51, RAD52, RAD54, BRCA1, and BRCA2. One of these, RAD51, is recruited by RAD52 to promote invasion of the broken DNA strands into an intact double-stranded homologous DNA duplex molecule. New DNA is synthesized. The ends are ligated by DNA ligase I and the interwound strands are separated, usually with no loss of genetic material (*26*).

The repair kinetics of DSBs after low-LET radiation are biphasic, with a fast (~0.5–1 h) and a slow component (several hours). A large fraction of the DBSs induced by low-LET radiation is repaired in the fast component, the duration of which is dependent on the cell line. The

repair kinetics of DSBs induced by high-LET radiation is generally slower than after X-rays and a larger fraction of the breaks remain unrepaired after long repair time (*27-30*). Residual damage after 24 h is often correlated to increased radiosensitivity (*31-32*).

The repair of DSBs is essential for cell survival and maintenance of the genomic integrity. If DSBs are left unrepaired, genetic material is lost during the following mitosis. Alternatively, wrong DNA ends can be combined during the rejoining process leading to different types of chromosomal aberrations. Also, NHEJ after radiation induced DSBs always results in some loss of genetic material since the ends must be trimmed to permit ligation. This may not be a problem because most of the bases are not coding for a gene product, but if it occurs in a coding sequence this may lead to mutations. If these events are not lethal, surviving cells that are genetically instable may evolve. Years later, such subclones with high proliferative capacity may develop into clinical malignancy (*33*).

Checkpoint Control

In cooperation with DSB repair, arrest in cell cycle progression is an important response to DNA damage, allowing proliferating cells to pause and repair lesions. Cell cycle checkpoints halt proliferation of damaged cells and are essential for maintenance of the genomic integrity by preventing mitosis in the presence of DNA damage. Cells are equipped with an advanced signaling system to induce cell cycle arrest. If the damage is too severe to repair, the cell can instead respond by signaling to undergo apoptosis. Depending on the position in the cell cycle at the time when the damage occurs, the cells will either be arrested in the G_1 phase (G_1/S checkpoint), slow down in S phase (S phase checkpoints), or be arrested in G_2 (G_2/M checkpoints). Compared with low-LET radiation, irradiation with high-LET radiation results in a more pronounced and sustained delay in both G_1 and G_2 compared to low-LET irradiation (*34-35*).

When a DSB occurs, the cell will respond through the activation of systems that detect the lesion, and trigger a cascade of various downstream events driven by the protein kinase ataxia telangiectasia mutated (ATM), which is recruited to and activated at DSB sites. Once activated, ATM will phosphorylate various substrates including checkpoint kinase 2 (Chk2),

BRCA1, NBS1, and p53, all important in cell cycle control systems. Checkpoint kinase 2 is activated through phosphorylation at threonine 68 (*36-40*).

Radiation Response in Proliferating and Resting Cells

Consequences of ionizing radiation, such as chromosomal damage or cell death, become manifest after subsequent cell divisions, and therefore can be observed early after exposure in proliferating tissues with a high cellular turnover rate. By contrast, the damage of tissues with a low fraction of dividing cells will be visible at a later time after irradiation. This is the reason why we can observe late side effects many years after radiotherapy and accidental radiation exposure.

The sensitivity of mammalian cells to low-LET radiation varies during the cell cycle. Cells in mitosis followed by G_2 are known to be the most radiosensitive, while cells in late S phase are the most radioresistant (*41*). This variability in radiosensitivity has also been observed *in vivo* in crypt cells in the mouse jejunum (*42*). Cells irradiated in late S phase are thought to repair lesions more properly, which is explained by the fact that both NHEJ and HRR are available. In contrast to low-LET radiation sensitivity, it is generally considered that the sensitivity to high-LET radiation is cell cycle-independent (*43*), although there are some reports of a differential response due to differences in cell cycle position and differences in the repair capacity have been reported (*44-47*).

The tissues in our body consist substantially of resting cells while tumors predominately consist of proliferating cells. Therefore, the discrepancy in radio response between proliferating and resting cells may be of large importance in a clinical situation where both tumors and surrounding normal tissue will be irradiated, especially when using new radiation qualities.

Influence of Chromatin Structure

In eukaryotic cells, the DNA is packaged and arranged together with histone proteins in various structures, to form chromatin. The elementary repeating units of chromatin are called nucleosomes, composed of 146 bp DNA wrapped, almost twice, around an octamer of histone proteins (H2A, H2B, H3, and H4) (*48*). The three dimensional chromatin structure changes naturally during the cell cycle, from unwinded DNA in S phase to tightly compacted chromatin in mitosis. Open chromatin structures are associated with increased transcriptional activity and are thought to be more sensitive to ionizing radiation, while dense chromatin is associated with inactive regions in the genome (*49*). The chromatin organization can be modified *in vitro* by treatment with high salt concentrations and modulation of the magnesium concentration. The architecture of the chromatin can be reversibly modified by promoting acetylation/deacetylation of histones to result in a more open/more compacted chromatin conformation (*50*). Clinically, histone deacetylase inhibitors have been suggested to suppress tumor invasion as a result of growth arrest and apoptosis (*51-52*).

The chromatin organization is an important factor in the induction of DSBs and other DNA lesions. Compacted chromatin is an effective radical scavenger, protecting from free radicals produced by ionizations of water molecules in proximity to DNA (*17*). By contrast, an open chromatin structure leads to higher yield of DNA damage (*17, 53*). Since the indirect effect is not as prominent after high-LET irradiation as after low-LET irradiation, this protective effect is of less importance using high-LET radiation. Also, presence of chromatin proteins is responsible for the non-random distribution of DSBs, typically found after high-LET irradiation (*53*). Recently, it has been shown that repair kinetics is dependent on the chromatin compactness, with a more efficient repair in open regions (*49*). Therefore, it can be reasoned that compact chromatin may be protected from induction of DNA damage but on the same time more difficult to repair.

Use of High-LET Radiation

In clinical radiotherapy the therapeutic index, i.e the distance between the tumor cure probability and normal tissue complication probability curves is small, since energy from ionizing radiation is transferred identically to tumor and normal cells. Therefore, in radiotherapy it is important to keep the absorbed dose to surrounding healthy tissue to a minimum while delivering enough energy to the correct target.

During recent decades high-LET irradiation has been introduced in external beam therapy using accelerated heavy ions (*54*) but also experimentally in internal radionuclide therapy (*55-56*). The advantages of high-LET radiation over low-LET radiation are the favorable dose distribution between tumor cells and normal cells, and less dependence on tumor hypoxia, dose rate and cell cycle position (*3, 43, 57*). At the same time, the biological effects in the cells are more severe after high-LET radiation, resulting in high RBE.

In recent years, radioimmunotherapy (RIT), i.e. treatment with monoclonal antibodies directed against a specific tumor antigen and labeled with a radionuclide, has been an alternative for internal radionuclide therapy, in most cases using beta emitters. Due to the relatively long range of these electron tracks, beta-RIT is not suited for treating small tumor cell clusters and isolated malignant cells. However alpha-emitting radioconjugates offer a better dose deposition due to the short alpha particle track, in the range of 50–100 µm.

Astatine-211 is one of few available α-emitting radionuclides. It has a suitable half-life that has made it interesting for RIT. It has been used by our group (www.tat.gu.se) in several preclinical studies and recently in a phase I study on ovarian cancer (*58*). It has also been used for evaluating toxicity, pharmacokinetics and efficacy of glioblastoma (*59*). Other clinical applications using α-particles are ^{213}Bi-RIT for leukemia (*60*) and melanoma (*61*) and unconjugated ^{223}Ra as a boneseeking nuclide for bone metastsases (*62*).

Since high-LET irradiation is being gradually introduced clinically it is of outmost importance to increase our knowledge of cellular radiation effects to improve treatment efficacy. Knowledge of the biological effects after high-LET irradiation is also of high interest when it comes to radiation protection issues. As described above, there is a correlation between

ionizing radiation and cancer, which is one of the leading causes of death. Human cells are exposed to ionizing radiation from natural background sources in our environment and the largest proportion of this comes from isotopes of radon in the ground and buildings. Radon is an α-particle-emitting radionuclide and when it is deposited internally, primarily in the lungs, it can be very hazardous. Evaluating biological effects of high-Z energy particles is also of interest for astronaut health concerns since more extended space explorations are planned in the future.

Present Investigation

This work was initiated with the aim of revealing the radiobiological effects of the α-particle emitter ^{211}At. For this purpose, normal cells were irradiated and the effects on the level of inflicted DNA damage, cellular response, and biological consequences were studied to increase our knowledge about this promising radionuclide.

AIMS

The main aim of the present work was to determine the relative biological effectiveness of α-particles from [211]At in normal cells of different proliferating status for endpoints ranging from DNA damage to cellular response and cell death.

The specific aims in each paper were:

I   To determine the induction yield and size distribution of DSB fragments in normal fibroblasts.

II   To study the induction of DSBs and clonogenic cell survival in relation to cell cycle position in synchronized cells.

III   To investigate repair of DSBs and activation of cell cycle arrests in irradiated normal fibroblasts of different proliferation status.

IV   To study the formation of chromosomal damage and delays in cell cycle progression in irradiated normal fibroblasts of different proliferation status.

MATERIALS AND METHODS

Cell Lines and Culture Conditions

In paper I, III and IV human diploid foreskin fibroblasts (HS 2429 cells) were used to represent a normal cell type with normal functions in regard to repair, arrests and proliferation. HS 2429 cells are contact inhibited, anchorage dependent and have a definite life span. These cells can be manipulated to obtain cultures with different proliferation status. In paper II, Chinese hamster lung fibroblasts (V79–379A cells) were used since they are able to form colonies and can be synchronized more efficiently than HS 2429 cells. Both cell lines were cultured at 37°C in a standard incubator in humidified air. The passage number was kept as low as possible, ranging from 8 to 15 (HS 2429 cells), and between 2 and 10 from the time of delivery (V79–379A cells).

When induction and repair of complex DNA damage were investigated, cells in culture were labeled with ^{14}C-thymidine prior to irradiation. Cells were irradiated at 2°C to avoid DNA repair in PBS or in serum free medium either as monolayers (paper I, III, IV) or as single cell suspensions (paper II). When the influence of temperature was investigated (paper I), the cells were irradiated in PB+ (nuclear monolayers) and in PBS (intact cells) at 2°C or 37°C.

Synchronisation of Cells

In paper II, V79–379A cells were treated with mimosin to achieve a synchronized population i.e. cells enriched in a specific position of the cell cycle. Mimosine is a relatively non-toxic reversible inhibitor of fork elongation that stalls replication in early S phase (*63*). Asynchronous cells were first accumulated in G_1 by serum starvation, followed by treatment of mimosine to block cells very early in S phase, halting cell proliferation. Removal of mimosine then allowed cells to proceed into S phase as a synchronized population. Stalled replication caused by mimosine has been shown to induce DNA lesions (*64*). Indeed, the control samples after treatment with mimosine was 100% higher compared with control

samples from asynchronous cells not treated with mimosine. However, individual control values were subtracted from each irradiated sample. To achieve cells in mitosis, mitotic shake-off was used in combination with serum starvation and treatment of mimosine. Mitotic shake-off is based on that cells progressing into mitosis become round and have fewer points of attachment with the culture vessel, which makes them easy to shake off and collect.

Flow cytometry analysis was used to optimize times, specific for each cell cycle phase, after release from mimosine treatment and times to achieve cell populations with the highest fraction of cycling cells as possible. The fraction of cells in mitosis was verified after May-Grünwald Giemsa staining, revealing a high percentage of cells in different stages of mitosis.

In paper III and IV, both stationary and cycling cell populations of HS 2429 fibroblast were used. To achieve stationary cells in G_0/G_1, cells were seeded in complete medium and grown to confluency before the time of irradiation. Populations of cycling cells were achieved by seeding cells at low cell density 24–28 h before irradiation. To obtain cells with different proliferation status, this procedure is more advantageous than synchronization with mimosine because no chemical manipulation of the cells is included and may therefore better reflect the normal situation in tissues.

Irradiation

Low-LET Irradiation

Low-LET irradiation was performed with a roentgen tube suited for contact therapy and with γ-rays from ^{60}Co. The mean absorbed dose from X-rays was determined from depth-dose curves developed for clinical use.

Table I. Beam properties

Radiation	Voltage (kV$_p$)	Filtration (mm Al)	Collimator/ Radiation field (cm)	Dose rate (Gy/min)	Focus/Source Target distance (cm)	Paper
X-rays	70	1.25	7×7	11.6	10	I
X-rays	100	1.7	7×7	13.5	10	II and III
X-rays	100	1.7	Ø12	1.46	30	II-IV
^{60}Co			10×10	1.09	80	I

High-LET Irradiation

Throughout this work, α-particles from ^{211}At were used as high-LET radiation. Astatine-211 is a halogen with element number 85 and decays with a half-life of 7.2 h. It has two branches of decay, resulting in 100% α emission. It disintegrates with 58% probability through electron capture to ^{211}Po, which in turn emits an α-particle of 7.45 MeV, with a half-life of 0.52 s. The other branch disintegrates with 42% probability through direct emission to ^{207}Bi, resulting in an α-particle of 5.87 MeV. Both branches end in stable ^{207}Pb. The average range of the α-particles is 65 μm in tissue, corresponding to a few cell diameters, and with mean LET of ~110 keV/μm (Fig. 1).
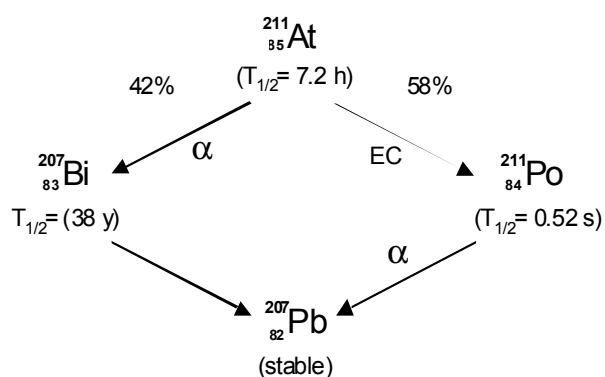
Figure 1. *Simplified decay scheme for Astatine-211 (^{211}At).*

Astatine-211 was produced by the ^{209}Bi(α,2n)^{211}At reaction in a cyclotron at the Positron Emission Tomography and Cyclotron Unit, Rigshospitalet, Copenhagen, Denmark, by irradiating a ^{209}Bi target with ~28 MeV α-particles. The target was isolated and transformed into a chemically useful form by a dry-distillation according to a protocol described by Lindegren *et al*. (*65*). As free astatine has been shown to bind to cells in suspensions to a varying degree (*66*) ^{211}At was labelled to monoclonal antibodies, MX35 F(ab´)$_2$ fragments (paper I) and Trastuzumab (Herceptin) (paper II-IV) using the reagent *N*-succinimidyl-3-(trimethylatannyl)-benzonate, as described earlier (*67-68*). MX35 is an antibody directed towards an antigen on the cell surface on ovarian carcinoma cells and was used in Göteborg clinical trials with patients with intraperiotenal growth of ovarian cancer. Trastuzumab is targeting the human epidermal growth factor receptor HER2/neu and is used in therapeutic treatment of breast cancer. However, the antibodies were not specific for the cell lines used here and were used only for stabilizing the astatine atom and preventing adhesion to plastic surfaces. In this work no binding or uptake of ^{211}At was desired for dosimetric reasons, hence the cellular uptake was measured using centrifuge tube filters (*66*) and was found to be less than 0.3%. Immediately after irradiation cells were washed 3 times in PBS or serum free medium. To ensure that no activity remained, all flasks and tubes were measured after the rinsing procedure in an ionizing chamber calibrated for high activities and a NaI(Tl)-well detector for low activities.

The absorbed dose to the cell nucleus was calculated from the equilibrium dose to the solvent, D$_{eq}$, given by:

$$D_{eq} = \frac{\tilde{A}nE}{m} \quad \text{and} \quad \tilde{A} = \int_0^T A_0 e^{-\lambda t} dt \tag{1}$$

where A_0 is the activity (Bq) added to the cell solvent, nE is the mean energy per transition (Gy Kg Bq^{-1} s^{-1}), λ is the disintegration constant, t is the time of irradiation and m is the mass of the solvent calculated from the density of the added volume. In cells irradiated as monolayers, the absorbed dose to the cell nucleus was approximated to half of the equilibrium dose, i.e. 0.5 D$_{eq}$, with the assumptions that the cells were adherent and the dose distribution homogenous in the solvent. In paper II, when cells were irradiated as single cells in suspensions, the cell nuclei will almost receive the same dose as the surrounding solvent, D$_{eq}$.

A correction of the mean absorbed dose to the nucleus was done according to a microdosimetric model that allows calculation of single-hit and multi-hit distributions of specific energy (*69*). Considering the cells to be isolated and spherical with a cell radius of 7 μm and a radius of cell nucleus of 5 μm, the absorbed dose to the cell nuclei was estimated to 0.95 D_{eq}.

## Fpg Enzyme Treatment to Assess Clustered Damages

The induction of clustered damage after irradiation was quantified in asynchronous V79–379A cells with PFGE and fragment analysis (paper II). Clustered damages within 10–20 bp were assessed by incubation with a base excision repair endonuclease post-irradiation to transform bistranded clustered damage into DSBs. Lysed cells were treated with Formamidopyrimidine-DNA glycosylase, Fpg, for 1 h in 37°C. Fpg recognizes oxidized purines and cleaves the strand at cluster sites inducing strand breaks that appear as additional DSBs if located on opposite DNA strands (*70*).

Pulsed-Field Gel Electrophoresis

Induction and repair of DNA DSBs were measured by pulsed-field gel electrophoresis (PFGE) in combination with fragment analysis which is a well established method for measurement and analysis for DNA DSBs.

PFGE was developed 1982 by Schwarz and Cantor *(71)* as a tool for separation of DNA fragments from approximately 10 kbp to 10 Mbp in size. The principle is that when the negatively charged DNA fragments are loaded into an agarose gel, they will migrate under an electric field at a speed that is inversely proportional to the size of the fragments. By varying the concentration of agarose, field strength and pulse duration, DNA fragments of different sizes can be separated. The concentration of the agarose affects both the resolution and the mobility of the DNA fragments. By periodically changing direction of the electric field the DNA is forced to change direction during electrophoresis and different sized fragments begin

to separate from each other. Longer pulse time and weaker electric fields lead to separation of larger DNA fragments.
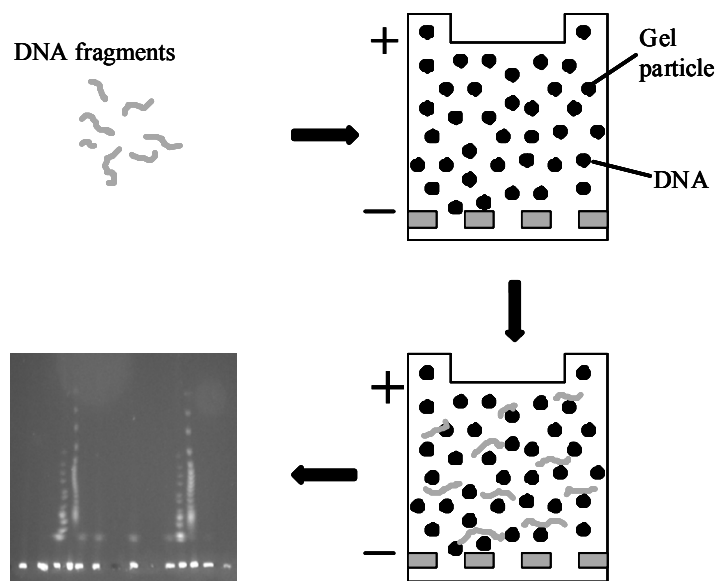

Figure 2. Illustration of PFGE and fragment analysis. DNA samples are loaded into a gel containing a matrix of agarose. The negatively charged DNA fragments move toward the positve electrode in a rate proportional to their length and will therefore be size separated. After staining with a fluorescent dye, DNA of different lengths can be identified using specific size markers.

Conventionally, PFGE is used to calculate the number of DSBs from FAR values. The FAR value, *Fraction of Activity Released*, describes the relative amount of ^{14}C-labeled DNA that migrates through the gel during electrophoresis and correlates in a non-linear way with radiation dose. FAR values can be converted into DSB under the assumption of randomly distributed DSBs along the DNA helix (*72*). This conversion is suitable after low-LET irradiation but in the case of high-LET irradiation, however, this assumption is not correct. Instead, another approach for determining the number of DSBs is needed, using further separation of fragments. DNA markers, well characterized in size, are loaded together with the samples in the gels and used to localize separated fragments of specific sizes. The total amount of DSBs is then calculated by summarizing DSBs in all fragment size intervals. The method is called fragment analysis and can also be used to determine the distribution of fragments of different sizes along the DNA.

In this work, two different electrophoresis protocols were used being optimized for separation of DNA fragments <1.1 Mbp and 1.1–5.7 Mbp, respectively. The calculations of DSBs induced were done by fragment analysis from the FAR values in each size segment. For this, lanes of migrated DNA were sliced in segments using three different size standards: Lambda DNA ladders, *Saccharomyces cervisiae* chromosomal DNA, and *Schizosaccharomyces pombe* chromosomal DNA. The number of fragments was calculated by dividing the fraction of ^{14}C-incorporated DNA in a gel segment, measured by a liquid scintillation counter, with the average fragment size in that segment.

Today, the most widely used method to determine DSB induced by ionizing radiation is detection of phosphorylation of the histone H2AX, called *γ*-H2AX in its activated form, which can be visualized within individual cells as distinct foci using antibodies specific for its phosphorylated form. The advantage with *γ*-H2AX over PFGE is the possibility to investigate effects of clinically relevant doses. One problem with the detection of DSB with *γ*-H2AX is the poor resolution of correlated DSB after high-LET radiation and therefore, the number of DSB will be underestimated in high-LET-irradiated cells. One of the main aims of this work was to estimate RBE for α-particles from ^{211}At and therefore, detection of DSBs was made using PFGE and fragment analysis instead of *γ*-H2AX foci quantification.
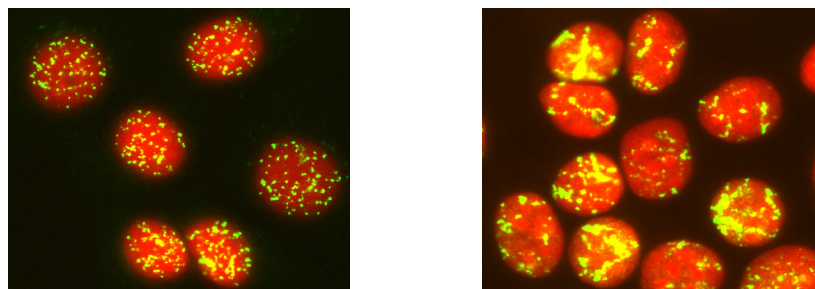
Figure 3. *γ-H2AX-foci (green) in propidium iodide stained cell nuclei in cells receiving 1 Gy X-rays (left) or 1 Gy ^{211}At (right).*

Micronuclei Assay

Radiation-induced chromosomal damage can be detected by investigating the formation of micronuclei (MN) in living cells. MN are formed of acentric fragments or whole chromosomes that have not been incorporated into daughter nuclei at mitosis and it is assumed that a cell carrying MN has lost its clonogenic capacity (73). The most widely used method for scoring MN is the cytokinesis-block micronucleus assay, which is a rapid and simple method that can be used at clinically relevant doses. In this assay, the fraction of MN is scored in binucleated cells when blocked from performing cytokines by cytochalasin B. The advantage with the use of cytochalasin B is that MN are scored only in binucleated cells, i.e. cells that have undergone one mitosis after irradiation, enabling reliable comparisons between cell populations that differ in their cell division kinetics. However, in this work MN formation was detected in cell cultures not treated with cytochalasin B due to its toxicity. HS 2429 cells, irradiated as confluent cultures had to be split directly after irradiation to prevent contact inhibition of cell division, a process for which a cytoskeleton drug is very toxic. Therefore, the number of MN formed after irradiation in the whole cell population was scored. 48 and 72 h post-irradiation, cells were fixed and stained with DAPI. Nuclei were then scored blind for MN using the criteria described by Fenech *et al. (74)*. The mitotic index, determined by detection of binucleated cells in the presence of the cytokinesis inhibitor cytochalasin B, was in the same range, 33% and 22%, for cycling and stationary cells, respectively. In these experiments cytochalasin B was added 6 hours after plating.

Measurements of Cell Proliferation

In this work, the cellular capacity to proliferate after irradiation was determined using two different assays: clonogenic assay and growth assay. These two methods differ in that the growth assay measures the total biomass and the proliferation of the entire cell population whereas the clonogenic assay measure the capacity of an individual cell to divide infinite times.

In paper II, cell survival of irradiated V79–379A cells was assessed by the clonogenic assay in which the ability of a single cell to form a colony exceeding about 50 cells, representing 5–

6 divisions, was determined. Asynchronous cells, cells in G_1, early, mid and late S phases and mitotic cells were irradiated as single cell suspensions with ^{211}At or X-rays. Following irradiation, cells at low density were seeded and incubated at 37°C for four days. The resulting number of colonies, consisting of at least 50 cells, was scored and the surviving fraction (SF) was calculated.

The growth kinetics in HS 2429 cultures after irradiation was determined by measuring the total cell number after crystal violet staining (paper IV). Crystal violet is a dye that binds to the cells resulting in optical density proportional to the cell number. Immediately after irradiation the cells were seeded in 96-well plates and incubated 1–15 days. After being fixed and stained with crystal violet, the optical density of dye extracts was measured using a micro plate reader. This assay is a suitable method for determination of radiation effects when cells do not form colonies and the clonogenic survival assay is not possible to use.

Measurements of Cell Cycle Arrests

Delays in cell cycle progression were examined by measuring cell cycle distributions with flow cytometric analysis after propidium iodide staining 0–72 days (paper III) or 0–22 days (paper IV) after irradiation. The percentage of cells in G_0/G_1, S phase and G_2/M was estimated by calculating the area under the DNA histogram assuming a Gaussian function.

In paper III, phosphorylation of the checkpoint kinase Chk2 at Threonine 68 was used as an indicator for cell cycle arrest activation 0–120 h post-irradiation. Cells cultured on chamber slides were fixed prior to incubation with a primary antibody binding to the phosphorylated Chk2, followed by incubation with a FITC-conjugated secondary antibody. The number of Chk2-foci in individual nuclei was scored blind using fluorescence microscopy.

Modulation of Chromatin Structure

In paper I, intact cells were chemically modulated into a structure defined as nuclear monolayer by permeabilizing the cell membrane with the ionic detergent Triton X-100. After this treatment the nucleus was depleted of all soluble scavengers. Intact cells and nuclear monolayers differ in that the DNA in nuclear monolayers lacks the protective effect of these molecules surrounding the DNA, while the chromatin conformation remains mainly unchanged.

In paper IV, the chromatin structure was modified by treating cells with the histone deacytelase inhibitor trichostatin A (TSA) that prevents deacetylation of histones (*50*). The molecular effects of TSA are rapid and reversible since increasing levels of acetylated histone H3 on lysine 9 (Ac-H3K9) were seen already after 1 h exposure of 0.3 µM TSA while wash-out after four hours decreased the levels of Ac-H3K9 (data not shown). TSA was added to the cells four hours before irradiation and was removed prior to irradiation.

RESULTS AND DISCUSSION

Effects on DNA Damage Induction

Double-Strand Break Induction (paper I-III)

The number of DSBs induced in HS 2429 cells and V79–379A cells was investigated by fragment analysis to include short DNA fragments generated by correlated DSBs following exposure to high-LET radiation. The cells received 0–90 Gy X-rays or ^{60}Co, or 0–50 Gy [211]At. The induction yields are listed in Table II.

Table II. DNA DSB induction yields ± SEM.

Cell cycle phase	DSB/Gy per cell[a]		
	[211]At	X-rays	[60]Co
Stationary[b]	61 ± 3	20 ± 2	30 ± 3
Stationary[c]	19 ± 2	14 ± 1	
Cycling[c]	33 ± 3	17 ± 2	
Asynchronous[d]	79 ± 5	22 ± 0.3	
G_1 phase[d]	60 ± 6	20 ± 1	
S phase early[d]	110 ± 10	31 ± 5	
S phase mid[d]	130 ± 20	34 ±2	
S phase late[d]	120 ± 8	45 ± 1	
Mitosis[d]	390 ± 40	220 ± 50	

[a]Assuming 6×10^9 bp per diploid cell

[b]HS 2429 cells (paper I)

[c]HS 2429 cells (from repair study at t=0 in paper III)

[d]V79–379A cells (paper II)

The yields for DSBs induction for HS 2429 cells and asynchronous V79–379A cells were in the same range, or lower, as reported by several other authors using fragment analysis. For low-LET radiation, yields in the range 23–64 DSB/cell per Gy have been reported (*12, 53, 75-76*). After high-LET radiation, 41–73DSB/cell per Gy have been reported using α-particles with LET of 110 keV/µm or nitrogen ions with LET from 80 to 225 keV/µm (*12, 53, 75-76*). The deviations in yields between different studies may depend on LET, radiation quality and cell line used. The

yields for stationary HS 2429 cells after [211]At clearly differed between paper I and III, for unknown reasons.

To analyze the clustering of DSBs induced in stationary fibroblasts, the distribution of fragments of different sizes was studied and compared with a theoretical model that calculates the number of DSBs per unit length, assuming that DSBs are randomly distributed in the DNA (*72*). The normalized fraction of DNA fragments versus fragment size showed that the DSBs induced by high-LET radiation clearly deviated from the theoretical model (Fig. 4A). The non-random component was constructed by subtracting the theoretical distribution from experiment data (Fig. 4C). If the DSBs were randomly induced in the DNA the data would be a straight horizontal line. High-LET radiation induced an excess of shorter DNA fragments and a decrease of longer fragments, in accordance with other publications (*12, 77*). DSBs resulting in short fragments <121 kbp constituted of about 40% of the total number of DSBs induced by [211]At. Radulescu *et al*. (*53*) suggested that the organization of DNA into the chromatin fiber and higher order structures is responsible for the majority of non-randomly distributed DSBs induced by high-LET radiation. The distribution of DSBs induced by X-rays on the other hand, comported well with the theoretical model (Fig. 4B) and less than 3% of the total number of DSBs resulted from fragments <121 kbp.
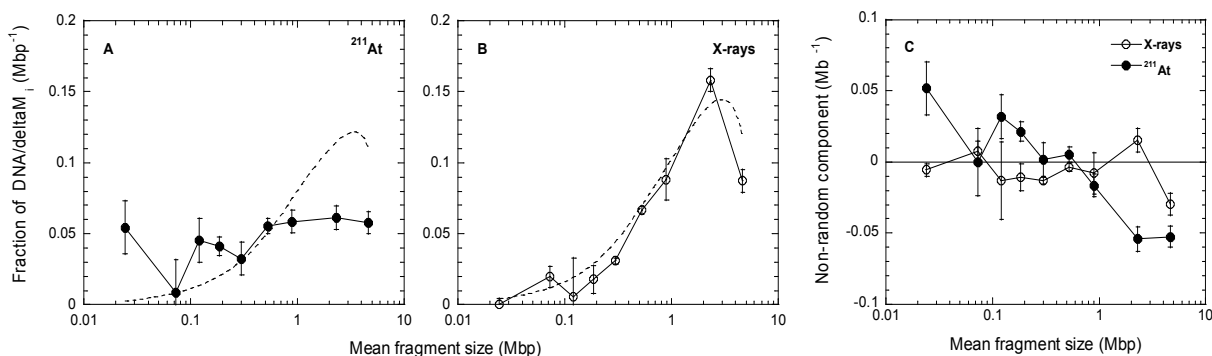
Figure 4. The normalized fraction of DNA fragments as a function of fragment size for stationary HS 2429 cells receiving 30 Gy [211]At (A) or 90 Gy X-rays (B). Dotted curves represent theoretical fragment distribution according to Blöcher's random breakage model for the same DSB frequency as obtained in the experiments. (C) the non-random component of the fragment distributions were constructed by subtraction of the theoretical distribution for the same DSB frequency as obtained from the data in (A) and (B).

In synchronized V79–379A cells, the number of DSBs increased when the cells progressed through the cell cycle (Table II). The yields per cell and corresponding cell cycle differences were similar to what has been demonstrated earlier for low-LET radiation. This cell cycle effect was not the result of lagging fragments containing replication forks, since this decreased mobility during electrophoresis was compensated for (*78-79*). One reason for the increased DSB yield during cell cycle progression is the increase of DNA content during DNA replication, but could also be a consequence of the chromatin structure. If the difference in DNA content was the only reason for variations of DSB induction between cell cycle phases, there would be only a two-fold increase of DSBs in mitotic cells. The induction yields showed that 6.6 and 11 times more DSBs were induced in mitotic cells relative G_1 cells irradiated with [211]At and X-rays, respectively. A similar finding has also been shown by Radford (*47*). He found a 3–4-fold increase of DSBs in mitotic cells compared with cells in early S phase measured with the neutral filter elusion assay. The large increase of DSBs in mitotic cells, compared to cells from other cell cycle phases could in part be explained by the increase of short DNA fragments. Fragment analysis showed a striking deviation from the random distribution in mitotic cells also for low-LET radiation. The contributions of short DNA fragments <121 kbp were 13% in G_1 cells and 80% in mitotic cells. The remarkable increase of short DNA fragments in mitotic cells is probably a consequence of the very compact chromatin organization. This indicates that fragment analysis, requisite for quantification of non-randomly induced DSBs, may be a necessary tool for DSB measurements, not only after high-LET radiation but also for low-LET under certain circumstances.

In summary, α-particles from [211]At were more effective in inducing DSBs in a non-random fashion, compared with X-rays. Induction yields varied depending on position of cell cycle phase at the time of irradiation after both [211]At and X-rays.

Induction of Clustered Damage (paper II)

The induction of clustered damage was investigated in asynchronous V79–379A cells and the yield for cluster induction was 26 ± 1.3 and 15 ± 4.4 clusters/cell per Gy for X-rays (0–75 Gy) and [211]At (0–50 Gy), respectively. Somewhat more clusters than DSBs were induced in X-irradiated cells (1.2 ± 0.05 clusters per DSB) in agreement with earlier reported findings (*80-82*). In contradiction, five times more DSBs than clusters were induce after [211]At. Only a few studies

investigating Fpg-clusters after high-LET irradiation in intact cells have been performed. The results from these studies show that none or less Fpg-clusters than DSB are induced after exposure to high-LET radiation (*16, 82-83*). The ratio between clustered damage and DSB tends to decline with LET and it appears as if non-DSB clustered damages are more dependent on the radical mediated indirect effect of ionizing radiation.

Effects on the DNA Damage Response

Repair of DNA Double-Strand Breaks (paper III)

The repair kinetics of DNA DSBs was investigated at a single dose, expected from DSB yields in paper I to induce the same amount of DSBs (30 Gy [211]At and 90 Gy X-rays). From Fig. 5 it is obvious that the repair kinetics differed between the two radiation qualities and three major distinctions can be mentioned. First, overall the repair kinetics was much slower after [211]At and second, more residual damage was detected after a repair time of 24 h post-irradiation. In stationary cells, 4% and 25% of the lesions remained unrepaired 24 h after X-rays and [211]At, respectively (Fig. 5A). Corresponding values in cycling cells were as high as 40% and 85%, respectively (Fig. 5B). Numerous studies on DSB repair have shown a slower rejoining and a larger amount of residual DSBs induced by high-LET radiation even after a long repair time (*27-30*). For example, Jenner *et al*. (*28*) reported that only 30% of the DSBs were rejoined after α-particles while >90% of those induced by X-rays were rejoined 3 h post-irradiation, at an absorbed dose of 40 Gy. Also, the repair kinetics measured by *γ*-H2AX foci fluorescence was dependent on LET with more persistent foci after long repair time (*84*). Groesser *et al*. (*85*) have shown that the foci numbers decreased faster after *γ* irradiation and returned to control levels 22 h post-irradiation while approximately 20–40% foci persisted after irradiation with Fe ions. The pronounced difference in the repair capacity between X-rays and [211]At, despite the dose adjustment, is probably due to the clustering of lesions along the α-particle track that may be very difficult to repair. The insufficient repair after high-LET radiation enhances the risk of failed or misrejoined DSBs, which in turn could lead to an increase of mutations, chromosomal damage and cell death. It is also possible that low- and high-LET radiation induce different amounts or ratios of DNA lesions in open versus compact chromatin, which may have consequences for DNA repair efficiency.

Third, an increase of DSBs was observed in [211]At-irradiated cells 1 h after onset of repair. In cycling cells, there were almost twice as many DSBs as promptly induced at t=0 (Fig. 5B). This increase of DSBs in [211]At-irradiated cells may depend on attempted repair of some radiation-induced sugar and base residues that can be converted to DSBs if located within a bistranded cluster.
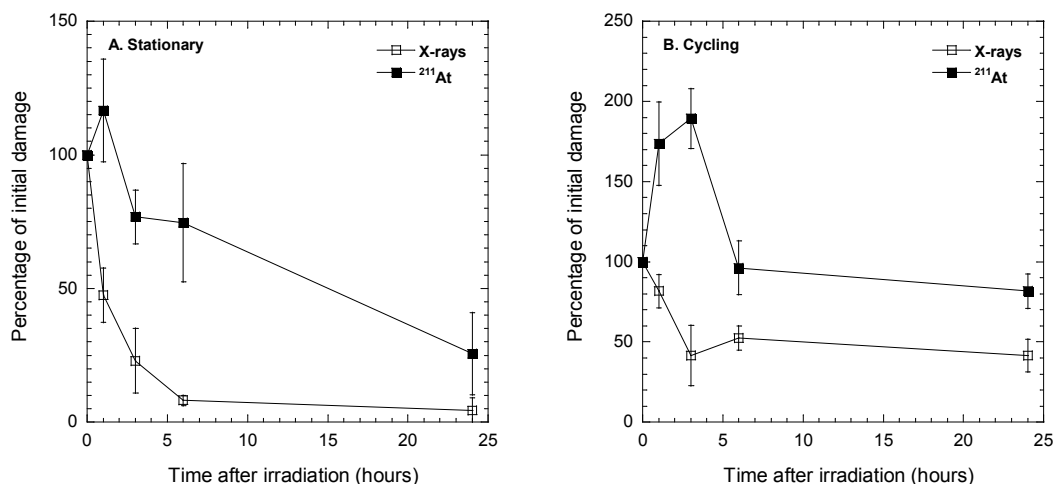
Figure 5*. Repair of DNA DSBs as percentage of initial damage as a function of post-irradiation incubation time. HS 2429 cells were irradiated either as a stationary cell culture (A) or as a cycling cell culture (B) and received 30 Gy [211]At or 90 Gy X-rays. Control values from unirradiated cells were subtracted from the results and the data represent the means ± SEM for at least three independent experiments.*

In stationary cells 96% and 75% of the promptly induced lesions were repaired 24 h post-irradiation after X-rays and [211]At, respectively (Fig. 5A). However, the repair of DSBs was much slower in cycling cultures than in stationary cell cultures, with 60% of the lesions repaired 24 h after irradiation with X-rays. In cycling cells irradiated with α-particles from [211]At only 15% of the promptly induced lesions were ligated (Fig. 5B). The slow repair kinetics in cycling cells was not caused by decreased mobility of S phase DNA in the agarose gel, since FAR values were normalized for this differential mobility. Fragment analysis showed that irradiation of cycling cells with X-rays induced more short DNA fragments compared to stationary cells. This increase of short DNA fragments may depend on the presence of cells in mitosis, with a distinct increase of short DNA fragments after irradiation as described above. Diverging differences in repair

kinetics between proliferating and resting cells have also been reported by other authors (*85-88*). For example, Hamasaki *et al*. (*88*) demonstrated a 1.5-fold increase of γ-H2AX foci in phytohemagglutinin stimulated lymphocytes one hour after X irradiation, compared to resting cells. Increased phosphorylation of H2AX in proliferating lymphocytes was also showed by Vilasova *et al*. (*86*).

It seems as if the DSB repair machinery prefers to repair isolated DSBs over lesions located in close proximity, since fragment analysis showed that the relative number of short fragments increased with repair time. In stationary cells, the fraction of DNA fragments <185 kbp increased from zero directly after X-irradiation to 50% after 3 h repair time. Corresponding numbers in cycling cells were 18% and 51%. Indeed, Wang *et al*. (*89*) have shown that very short fragments (<40 bp) prevent efficient Ku-binding, thereby decreasing DNA-PK$_{CS}$ recruitment to the two ends of the DNA fragments, resulting in NHEJ retardation. This may explain the insufficient repair after α-particles, primarily inducing correlated DSBs, and in cell irradiated as a cycling culture.

In conclusion, repair of DSBs induced by ^{211}At required longer time and resulted in higher proportion of unligated breaks after 24 h. There was a large difference in repair kinetics between cycling and stationary cells, with more insufficient repair in proliferating cells.

Effects of Radiation on Cell Cycle Progression (paper III and IV)

Detection of cell cycle arrests using immunofluorescent labeling of phosphorylated Chk2-foci showed a massive activation of Chk2 one hour post-irradiation, in both cycling and stationary cell cultures receiving 1 Gy ^{211}At or 3 Gy X-rays. Re-incubation at 37°C resulted in a decreased amount of foci by repair time, but even 120 h post-irradiation at least 50% more foci could be found in irradiated cells than in unirradiated cells (Fig. 6). In cycling cells, twice as many Chk2-foci remained after ^{211}At compared with X-rays, despite the dose adjustment, probably reflecting the inefficient repair in cells irradiated with ^{211}At. In stationary cells, a difference between the radiation qualities was first seen 48 h post-irradiation with about 1.5 times more foci after α-particles. The difference between cycling and stationary cells was more pronounced after α-particles with a two-fold increase of Chk2-foci 24 h and 48 h post-irradiation. After X-rays only small differences were observed with no consistent trend.
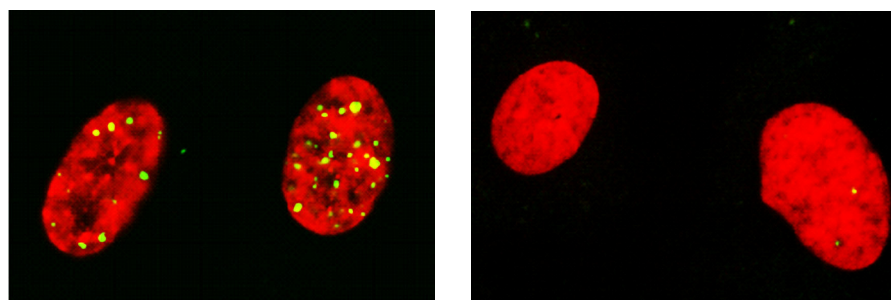
***Figure 6**. Photographs of Chk2-foci (green) in cell nuclei stained with propidium iodide receiving 1 Gy ^{211}At (left) or in unirradiated cells (right), 48 h post-irradiation.*

Detection of radiation induced cell cycle arrests using flow cytometic analysis showed a substantial arrest in G_2/M in cycling cells irradiated with α-particles from ^{211}At, 24–72 h post-irradiation (Fig. 7B). In contrast, no significant difference from control cells in cell cycle distribution could be observed after X-rays (Fig. 7B), albeit the higher dose.
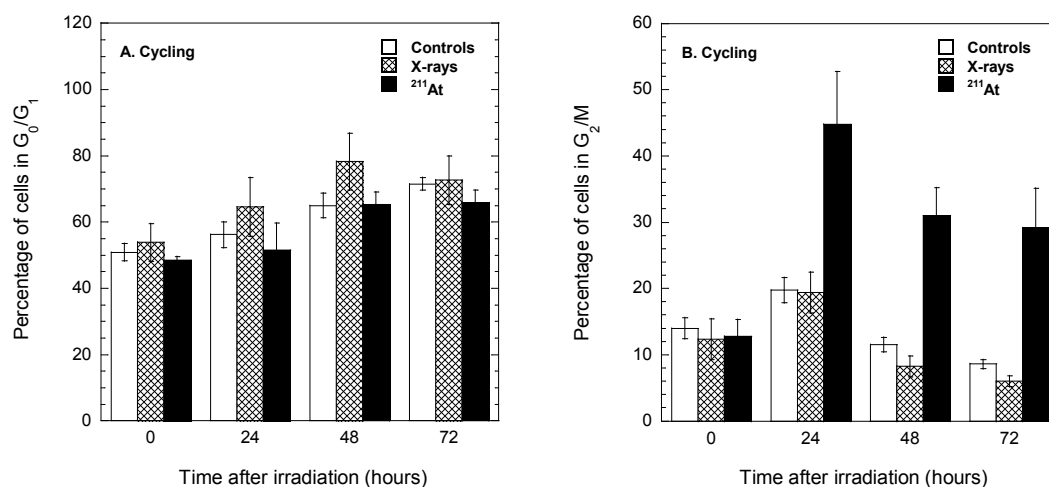
***Figure 7**. Cell cycle distributions in cycling HS 2429 cells irradiated with 1 Gy ^{211}At or 3 Gy X-rays, 0–72 h post-irradiation. The figures show percentage of cells in G_0/G_1 (A) and in G_2/M (B). Data represent the means ± SEM from two or three independent experiments.*

When cell cycle distributions were analyzed in a long time follow-up 0–22 days after irradiation, both [211]At and X-rays resulted in cell cycle progression disturbances corresponding to what was found 24–72 h after irradiation. Irradiation of cycling cells with [211]At resulted in a substantial and persisted accumulation of cells with about twice as many cells in G_2/M compared to unirradiated cells (Fig. 8A). After exposure to X-rays (3 Gy), only a minor accumulation of cells in G_2/M was observed (Fig. 8B). No effect on cell progression was observed in cells receiving 1 Gy X-rays.
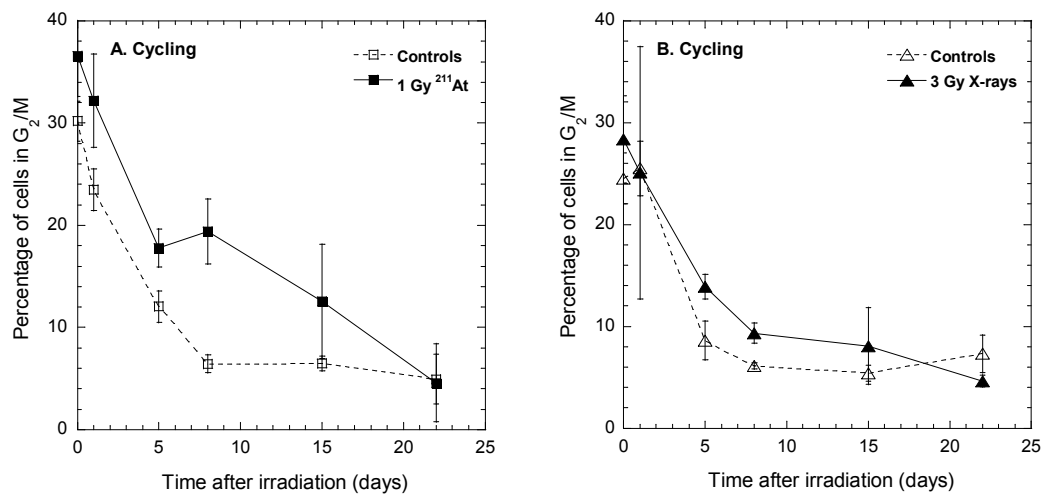
Figure 8. *Percentage of HS 2429 cells in G_2/M in cycling cell cultures 0–22 days after irradiation with [211]At (A) or X-rays (B). Data are the means ± SEM from at least three independent experiments.*

Such drastic G_2/M arrest after α-particles is in accordance with presented data from others on G_2/M arrests induced by different high-LET radiations (*90-92*). Dose dependent G_2/M delays have been suggested earlier. For example, Raju *et al*. (*93*) reported that the delays of progression through G_2/M was dose dependent for both X-rays and α-particles and Lücke-Huhle *et al*. (*90*) showed that the number of cells arrested in G_2/M after exposure with heavy ions increased linearly with dose up to at least 75% of the maximum fraction of cells in G_2/M. Indeed, primary fibroblasts requires doses >200 mGy to activate G_2/M checkpoint. Further, Buscemi *et al*. (*94*) suggested that the checkpoint kinase Chk2 needs >19 DSBs to be activated, which is in the same range as the DSB induction yields presented here.

Stationary cells were arrested in G_0/G_1 after release of the contact inhibition at plating, regardless of radiation quality (Fig. 9A). Only 5–10% of the irradiated cells started to proliferate 24 h post-irradiation, while this percentage was much higher in control cells.
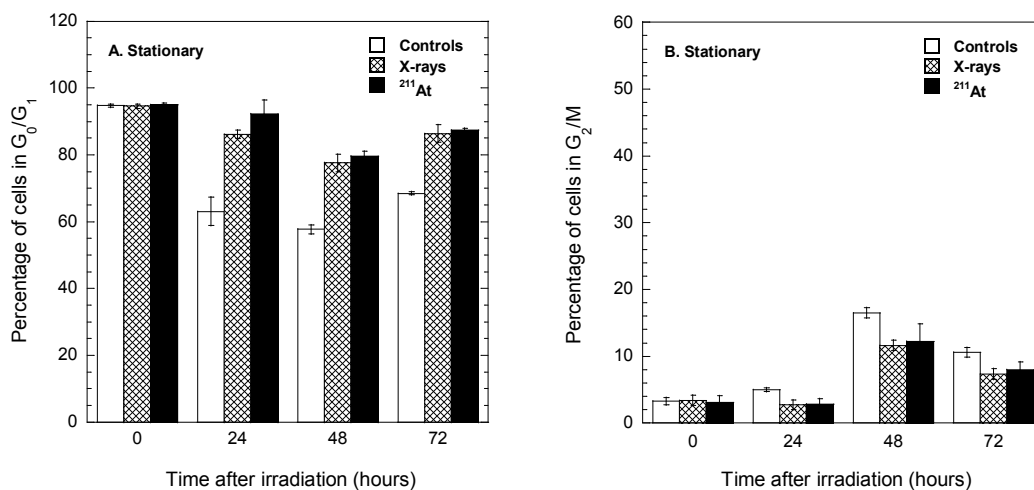
Figure 9*. Cell cycle distributions in stationary HS 2429 cells irradiated with 1 Gy ^{211}At or 3 Gy X-rays, 0–72 h post-irradiation. The figures show percentage of cells in G_0/G_1 (A) and in G_2/M (B). Data represent the means ± SEM from from two or three independent experiments.*

In accordance, stationary cell cultures investigated for long times (0–22 days) underwent a delayed cell cycle progression after release of the contact inhibition with a lower fraction of cells entering S phase at later time points after irradiation (Fig. 10). This was found after both ^{211}At (Fig. 10A) and X-rays (Fig. 10B), but was more prominent after α-particle exposure.

Figure 10. *Percentage of HS 2429 cells in S phase in stationary cell cultures 0–22 days after irradiation with ^{211}At (A) or X-rays (B). Data are the means ± SEM from at least three independent experiments.*

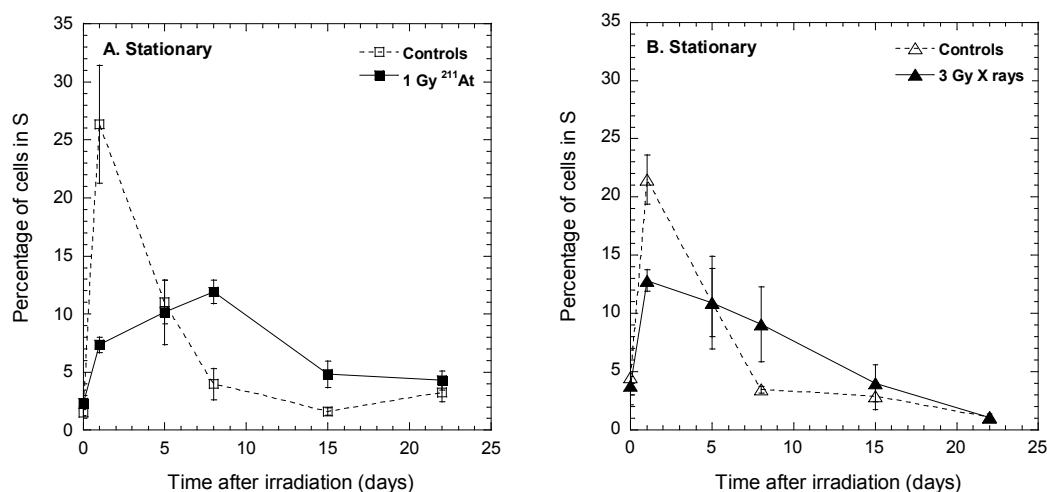Delays of the progression into S phase in non-cycling cells that are allowed to re-enter the cell cycle have been reported earlier (*95-97*). It is possible that a fraction of the cells irradiated as a stationary cell culture in G_0/G_1 and re-seeded immediately after irradiation do not start to proliferate but become permanently arrested. Indeed, Nasonova *et al*. (*95*) have shown that approximately 20% of irradiated normal cells were irreversibly blocked in G_1 following subculture and Tenhumberg *et al*. (*96*) have shown that only 25% of normal fibroblasts reached the first mitosis after exposure to low energy particles, supporting the data presented here. The arrest in G_1 provides extra time for the repair of DNA damage before the onset of replication and thus protects the cells against the effects of radiation.

Several studies have been performed on disturbances in cell cycle progression after irradiation with both low- and high-LET radiation. The predominant result from these studies was that an accumulation of cells in G_2 phase was observed after high-LET radiation (*90-93, 98*) , but also delays in G_1 and S phase have been demonstrated (*91, 96-97*). The duration of the block depends on radiation quality and dose (*92-93*). It appears as if the G1/S checkpoint is somewhat weaker than the G_2/M checkpoint. Indeed, Deckbar *et al*. (*99*) have shown that the G1/S checkpoint fails to prevent S phase entry of irradiated fibroblasts at early times after irradiation.

In summary, results from paper III and IV showed that cell cycle arrests were dependent upon the position of cells in the cell cycle at the time of irradiation. Cycling cells predominantly became arrested in G_2/M while stationary cells were arrested in G_1. Also, α-particles from [211]At resulted in more pronounced arrests than X-rays.

Chromosomal Damage (paper IV)

Chomosomal damage was studied by investigating the formation of MN in stationary and cycling HS 2429 cells, receiving 1 Gy [211]At, or 1 and 3 Gy X-rays. The formation of MN was dependent on radiation quality, dose and proliferation status. The amount of MN peaked at 72 post-irradiation, but also 120 h post-irradiation a large fraction of cells exhibited MN in the culture (data not shown). These remaining MN could be a consequence of both delayed cell cycle progression and of some MN formed after the second post-irradiation mitosis (*100*). When isodose was compared, [211]At was more effective in inducing chromosome damage. The average numbers of MN formed per cell after α-particles 72 h post-irradiation were 0.67 ± 0.04 and 0.47 ± 0.03 for cycling and stationary cells, respectively. At the same dose of X-rays, only 0.25 ± 0.02 and 0.12 ± 0.01 MN were formed in cells irradiated as a cycling and stationary cell culture, respectively. In cycling cells, increasing the dose of X-rays to 3 Gy resulted in the same amount of MN produced as after α-particles (0.69 ± 0.03) but this was not the case in stationary cells where the MN yield was much lower (0.28 ± 0.02). The complexity of chromosomal damage was more pronounced in cells irradiated with [211]At with more multiple MN per cell. Accordningly, in cells receiving 1 Gy α-particles from [211]At, the proportion of MN-positive cells with at least three MN 72 h post-irradiation was 27% and 22% in cycling and stationary cells, respectively. The corresponding numbers after 1 Gy of X-rays were only 9% and 2%. Increased complexity of chromosomal aberrations with increasing LET has been reported earlier (*101-102*). The increased complexity of chromosome damage after high-LET radiation is probably a consequence of correlated DSB and the inefficient repair thereof.
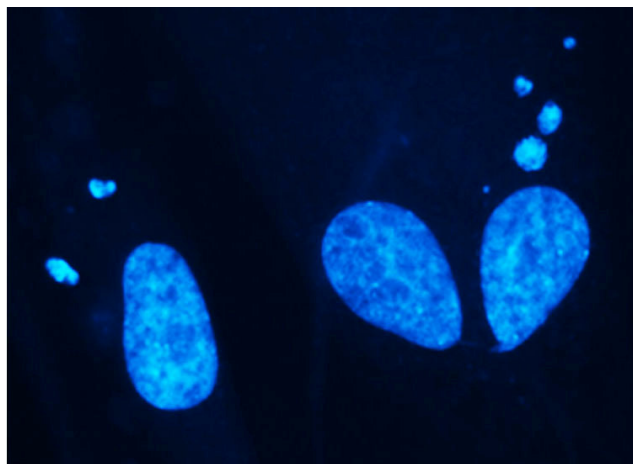
Figure 11. *Micronuclei in cells receiving 1 Gy α-particles from* ^{211}At *after 72 h incubation post-irradiation.*

It is obvious from the data presented here that cycling cells were more sensitive to ionizing radiation, resulting in a 40% higher yield of MN in cycling cells compared with stationary cells after ^{211}At irradiation. The difference was even more prominent after X-rays with 2–3 times more MN formed in cycling cells than in stationary cells and was not due to differences in mitotic events, biasing the evaluation. These data on differences due to proliferation status are in agreement with some earlier findings on MN formation after genotoxic stress in different cell cycle phases (*103-104*). In addition, Masunaga *et al.* (*105*) have reported that the frequency of MN in tumor cells inoculated in mice was lower in quiescent cells than for a mixed cell population after both irradiation of *γ*-rays and carbon ions. Indeed, they demonstrated a positive correlation between the magnitude of this proliferation status effect and increasing LET, a correlation very similar to what we found here using α-particles with LET 110 keV/μm. The increased amount of MN induced in cycling cells could depend on several mechanisms. First, it has been shown that cells encountering DNA damage after chromatin condensation in mitosis complete cell division in presence of DNA damage despite proper activation of the DNA damage response (*106*). Damages induced late in the cell cycle will therefore contribute to chromosomal aberrations detected as MN after mitosis. Second, it has been demonstrated that full G_1/S arrest and blockage of replication is established several hours after irradiation and is often poorly maintained, leading to increased chromosomal breakage observed later (*99*). Third, the G_2/M checkpoint cannot prevent cells from progression into mitosis in the presence of DNA damage (*99, 107*). It can be assumed that such leakage through the checkpoint arrests will influence cells already cycling to a larger extent since cells irradiated as confluent cultures in G_0/G_1 before

plating may have sufficient time to complete repair before onset of replication many hours later. Also, from DSB repair studies in paper III it is clear that the repair process was very inefficient in cycling cells with a high proportion of unligated breaks remaining after 24 h. Such amount of residual damage may lead to consequences in the form of chromosomal damage, as shown here.

In summary, cells irradiated with α-particles from [211]At exhibited more chromosomal damage than X-irradiated cells. Also, cycling cells had more MN compared with cells irradiated as stationary cultures.

Clonogenic Cell Survival and Cell Growth (paper II and IV)

The radiosensitivity in asynchronous and synchronized V79–379A cells was measured with the clonogenic survival assay. The experimental data from X-rays was fitted to the linear-quadratic model (LQ), and data from [211]At was fitted to an exponential curve. The surviving fractions (SF) were much lower after [211]At than X-rays in all cell cycle phases, as well as in asynchronous cells (Fig. 12). In asynchronous cells, the dose required to reduce the SF to 37% was 5.5 Gy after X-rays but only 0.67 Gy after exposure to [211]At. The SF after 2 Gy was 81% and 5.2% for X-rays and [211]At, respectively.

The clonogenic survival after both X-rays and [211]At was dependent on cell cycle position at the time of irradiation. After X-rays, the lowest survival was found in mitotic cells followed by cells in G_1 phase. Cells in late S phase were the most radioresistant of all phases investigated. The dose required to reduce the survival to 37% increased as cells progressed through the cell cycle and was 1.6 times higher in late S phase compared with G_1 cells. Corresponding value for mitotic cells was 0.8. Since the classical findings by Terasiama and Tolmach (*41*), this pattern of radiosensitivity after low-LET irradiation between cells in different position of the cell cycle has been reported by a number of investigators (*47, 108*). The radioresistance in late S phase can be explained by the fact that both non-homologous end joining and homologous repair may contribute to a higher DSB repair fidelity and consequently also to the increased radioresistance (*109*).

In contrast to what is generally accepted for high-LET radiation, results from paper II showed that irradiation with [211]At also resulted in differences in radiosensitivity between different cell cycle phases although variations were not as large as after low-LET radiation. Surprisingly, and in sharp contrast to X-rays, mitotic cells were most radioresistant after [211]At, where a 1.5-fold higher dose was needed to reduce the survival to 37%. A possible explanation could be that DNA may be unhit in some cells after α-particles, biasing the surviving fraction, as it is condensed in its most compacted and sorted form, occupying less volume in the nucleus than chromatin in other cell cycle phases. It should be remembered however, that is not a condition restricted to cells *in vitro*. The cell cycle effect was more prominent when determined at the absorbed dose of 2 Gy. The SF in mitotic and mid S phase cells was only 25% of the SF in G_1 cells. In late- and early S phases, the SF was 50% and 75% of the SF in G_1 cells, respectively.
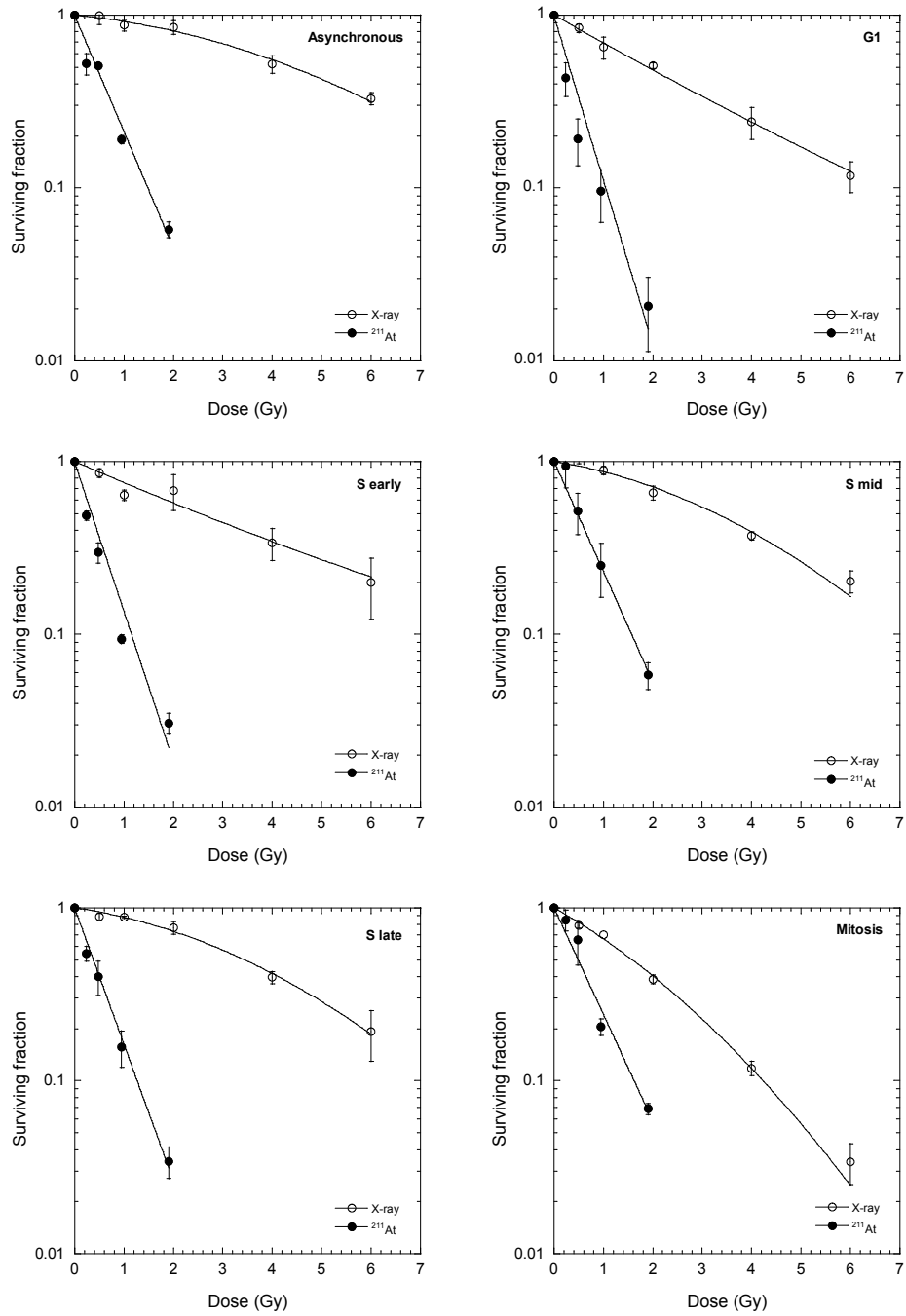
Figure 12. *Clonogenic cell survival in V79–379A cells after ^{211}At or X-rays, presented for asynchronous cells, G_1 cells, early, mid and late S phase cells and cells in mitosis. The results derive from at least three independent experiments ± SEM. Results from ^{211}At were fitted to an exponential curve and the results from X-rays to the LQ-model.*

In agreement with the result from the clonogenic survival assay, investigation of the proliferation of irradiated cells using a growth assay (paper IV) showed that α-particles from [211]At were more retarding than X-rays. Cycling cells were somewhat more growth inhibited than stationary cells with an almost absent regrowth regardless of radiation quality.

In summary, clonogenic survival was influenced by cell cycle position after both low- and high-LET irradiation. Also, the number of clonogenic cells and culture proliferation were reduced after [211]At, demonstrating that the radiation quality differences observed at earlier endpoints resulted in decreased survival of cells after irradiation with α-particle compared with X-rays.

Effects of Trichostatin A on Irradiated Cells (paper IV)

Effects of TSA-induced inhibition of chromatin deacetylation on the radiation-induced formation of micronuclei and cell cycle progression were studied. Compared to non-treated irradiated cells, TSA had an impact on cell cycle progression following irradiation, with an accumulation of cells in G_2/M in cells irradiated as cycling cultures after both [211]At and X-rays,. In stationary cells, an enhancement of the delay into S phase after 24 h post-irradiation in TSA treated cells was seen after [211]At but not after X-rays. In contradiction to this enhanced arrest activation, 10–27% less MN were formed 48 h post-irradiation in TSA treated irradiated cells, but this protective effect was reduced or abolished 72 h post-irradiation. In cycling cells, this could be explained by the fact that cells treated with TSA were arrested in G_2 after 24 h to a larger extent than non-treated cells, and therefore took longer time to enter the first mitosis after irradiation. Consequently, a higher proportion of TSA-treated cells could express chromosomal damage after 72 h compared with earlier times. There are some studies investigating a combined effect of TSA and radiation in cells showing that TSA treated cells were more radiosensitive than sham treated cells, with a higher impact on proliferating than stationary cells in agreement with the data presented here (*49, 110-111*). In conclusion, there was only a minor effect of inhibition of histone deacetylation which could be explained by the fact that there were no large heterochromatin regions in these cultured fibroblasts, as determined by transmission electron microscopy, and therefore, TSA may have only a limited influence on the radiation response.

Effects of the Irradiation Temperature (paper I)

Irradiation of nuclear monolayers after removal of soluble radical scavengers at 37°C instead of 2°C resulted in an increased number of induced DSBs. The resulting dose modifying factors, $DMF_{temp,}$ were 1.6 and 1.7 for ^{60}Co and ^{211}At, respectively. For low-LET radiation, a similar protective effect of low temperature on formation of DNA damage, correlated to the indirect effects of ionizing radiation, has been reported earlier (*112-113*). The increase of DSBs at 37°C found in this study also after high-LET irradiation is somewhat surprising. Possibly, irradiation temperature may influence the induction of other LET-dependent labile lesions on opposite strands, which could be converted into DSBs. No temperature effect was observed for intact cells receiving a single dose in this study of 20 Gy α-particles from ^{211}At, in accordance with earlier findings (*112-113*).

Relative Radiation Quality Effects

Below follows the biological effects of α-particles from ^{211}At, quantified as RBE values or radiation quality effects, for the different endpoints classified either as inflicted DNA damage, DNA damage response or biological consequences, investigated throughout this work.

Relative biological effectiveness for DSB induction was calculated from each corresponding dose response curve fit and values are listed in Table III. The RBEs for DSB induction in HS 2429 cells and asynchronous V79–379A cells were in the same range or higher than others have reported using the same method, with values between 1.2 and 1.8 for irradiations with LET of 40–225 keV/μm (*53, 75, 114*). Walicka *et al*. (*115*) have demonstrated almost a 10-fold higher DSB yield after DNA-incorporated ^{211}At compared with ^{125}I, using the neutral filter elusion assay. Interestingly, the RBE varied when the influence of cell cycle position was investigated with the smallest difference between the two radiation qualities found in mitotic cells. This may reflect the large increase of DSBs induced by X-rays, probably due to the chromatin organization as described above, as well as the larger dose inhomogeneity after high-LET irradiation of nuclei with condensed chromosomes.

Table III. RBE for induction of DSB and clustered damage.

	RBE$_{DSB}$	RBE$_{Clusters}$
Stationary[a]	3.1	
Stationary[b]	2.1	
Stationary[c]	1.4	
Cycling[c]	2.0	
Asynchronous[d]	3.5	0.59
G$_1$[d]	3.0	
S early[d]	3.4	
S mid[d]	3.9	
S late[d]	2.8	
Mitosis[d]	1.8	

[a]HS 2429 cells, reference radiation: 70 kV$_p$ X-rays (paper I)

[b]HS 2429 cells, reference radiation: ^{60}Co (paper I)

[c]HS 2429 cells, reference radiation: 100 kV$_p$ X-rays (paper III)

[d]V79−379A cells, reference radiation: 100 kV$_p$ X-rays (paper II)

There are to our knowledge only one published study on clustered damage in intact cells determining RBE after Fe ion irradiation, showing a value lower than unity in agreement with the value of 0.59 presented here (*82*). The low RBE can be explained by the increased influence of the indirect effect of ionizing radiation which is more dominant after low-LET than high-LET radiation.

Radiation quality ratios, calculated at expected isoeffect doses, for different endpoints of the DNA damage response were estimated for repair of DSBs, Chk2 activation and checkpoint arrests and are shown in Table IV. This means that the differences between α-particles and X-rays were even larger than numbers in the Table IV, since the dose was adjusted by a factor 3 to induce the same amount of DSBs in the two cases.

Table IV. Radiation quality ratios, after doses expected to induce the same amount of DSB, for different DNA damage response endpoints.

	Repair 3 h[a]	Residual damage 24 h[a]	Chk2 24 h[b]	Chk2 48 h[b]	G_0/G_1 arrest[c]	G_2/M arrest[c]
Stationary (HS 2429)	3.3	5.8	0.98	1.6	1.3	
Cycling (HS 2429)	4.6	2.0	2.3	2.0		8.4

[a]Percentage of initial damage determined after 30 Gy [211]At and 90 Gy X-rays.

[b]Calculated as the ratio of radiation effect between 1 Gy [211]At and 3 Gy X-rays.

[c]Calculated as the ratio of radiation effect, expressed as the absolute area deviation from control values in cell cycle distribution 0–72 h post-irradiation, between 1 Gy [211]At and 3 Gy X-rays.

Radiation quality ratios varied with repair time. In stationary cells, the ratio increased with repair time while the inverted relationship was found in cycling cells. This could in part be explained by the very efficient repair after X-rays in stationary cells while cycling cells had insufficient repair after both [211]At and X-rays, resulting in a lower ratio between the two qualities.

Radiation quality ratios for cell cycle arrest (Chk2 activation and arrest in G_0/G_1) were lower in stationary cells than in cycling cells (Chk2 activation and arrest in G_2/M). RBE values for α-particles between 4 and 9 for G_2/M delay have been reported by others (*90, 92, 116*). In those investigations these RBEs were determined either by comparing the doses required to produce the maximum value of cells in G_2/M at one specific time or by calculating the ratio of doses needed to increase the fraction of cells in G_2/M to a specific level. Only a few studies have estimated RBE for G_0/G_1 arrests, ranging from 0.8 to 3 (*96*), lower than those reported for G_2/M arrests, in accordance with the data presented here.

Radiation quality ratios for biological consequences of [211]At were determined for chromosomal damage, long-term cell cycle disturbances and for clonogenic survival (Table V).

Table V. Radiation quality ratios or RBE values for biological consequences.

Cell cycle phase	MN 72 h ratio	G_0/G_1 arrest[a]	G_2/M arrest[a]	$RBE_{37\%}$	SF_2 ratio
Stationary[b]	4.1	3.1			
Cycling[b]	2.7		13		
Asynchronous[c]				8.6	18
G_1 phase[c]				6.1	38
S phase early[c]				7.4	31
S phase mid[c]				6.1	13
S phase late[c]				7.9	28
Mitosis[c]				3.1	6.9

[a]Calculated as the ratio of radiation effect, expressed as the absolute area deviation from control values in cell cycle distribution 0–22 days post-irradiation, between 1 Gy [211]At and 3 Gy X-rays.

Radiation quality ratios for chromosomal damage, assessed as MN formation, was 2.7 and 4.1, 72 h post-irradiation for cycling and stationary cells, respectively. Several studies have determined RBE of α-particles for MN formation and values from 2.5 to 4.3 depending on LET, cell line used and proliferation status have been reported (*117-119*), supporting the values shown here.

The correlation between surviving fraction and radiation dose is not linear and therefore, RBE will vary depending on the level of damage investigated. RBE for 37% survival varied between 3.1 and 8.6 and SF_2 ratio between 6.9 and 38, depending on cell cycle phase. This demonstrates that at higher doses within the clinically relevant range, differences between radiation qualities will increase. Again, the RBE in cells irradiated in mitosis deviated notably from the other cell cycle phases. A few studies have been published on RBE determination of α-particles from [211]At at 37% cell survival, and values ranging from 1.6 to 12 have been reported for different cell types (*66, 115, 120*). Relative biological effectiveness of α-particles from [211]At determined *in vivo* has also been investigated. Bäck *et al.* (*121*) reported a RBE of 4.8 for growth inhibition of subcutaneous xenografts of human ovarian cancer cells implanted in nude mice, and Elgqvist *et al.* (*122*) reported RBEs of 3.4 and 5.9 for myelotoxicity, assessed as white blood cell counts, in nude mice after intravenous or intraperitoneal administration of antibody-labeled [211]At.

In summary, RBE values and radiation quality ratios of α-particles from [211]At were dependent on endpoint and dose level investigated, and varied depending on proliferation status.

SUMMARY AND CONCLUSIONS

To improve development of safe external and internal radiotherapy using high-LET radiation it is important to increase our knowledge of early DNA interactions, cellular responses and biological consequences of different high-LET radiation qualities. The aim of this thesis was to investigate radiobiological effects in cells after exposure to α-particles from ^{211}At, a promising candidate nuclide for α-RIT of isolated tumor cells and microscopic clusters, and X-rays in normal fibroblasts. *In vitro*, fibroblasts have been frequently used in radiobiology studies, and represent a normal cell type with functioning checkpoint arrest, repair and genomic surveillance signalling. In tissues, it is an abundant cell type in epithelium. In radiotherapy, irradiated fibroblasts often give rise to late consequences that can be observed months or years after treatment. In culture, fibroblasts can either be irradiated as a resting (stationary) population or as a proliferating culture after plating.

From the data presented here it is obvious that ^{211}At was more detrimental than X-rays. The induction of DSBs was higher with correlated breaks along the α-particle track. In cooperation with insufficient DSB repair, strong arrest activation was found with more Chk2-foci after ^{211}At compared with X-rays. Formation of chromosomal damage and effects on proliferation were also more prominent. Also, the clonogenic survival was reduced.

Interestingly, and in contrast to what is generally accepted, we found a cell cycle dependence for DSB induction and clonogenic survival in synchronized fibroblasts after irradiation with ^{211}At. For most endpoints studied here, a differential radioresponse between cells irradiated as stationary or cycling cultures was found, with cycling cells being more sensitive to ionizing radiation. Since irradiated tissue contains proliferating tumor cells as well as surrounding non-proliferative normal tissue, such differential radioresponse could be of great importance and should be further investigated.

ACKNOWLEDGEMENTS

I would like to thank

My supervisor **Kecke Elmroth,** for introducing me to the interesting field of radiobiology. Thanks for all your support on the way and for always being at hand. You have been an excellent supervisor.

My co-supervisors **Lars Jacobsson** and **Ragnar Hultborn,** for all support on the way

Karin Magnander, my roommate and group-member, for excellent collaboration, valuable discussions and your encouraging support during these years.

Madeleine Nordén Lyckesvärd, my roommate and group-member, for excellent help with my work.

Helena Kahu and **Ulla Delle,** for excellent help with my work.

The TAT-group, especially **Sture Lindegren** for supplying Astatine-211.

All other staff and former PhD students at the Laboratory of Oncology for creating a friendly atmosphere and a pleasant workplace.

My family

REFERENCES

1.   T. T. Puck and P. I. Marcus, A rapid method for viable cell titration and clone production with HELA cells in tissue culture: the use of X-irradiated cells to supply conditioning factors. *Proc. Natl. Acad. Sci. U. S. A.* **41**, 432-437 (1955).

2.   D. T. Goodhead, The initial physical damage produced by ionizing radiations. *Int. J. Radiat. Biol.* **56**, 623-634 (1989).

3.   J. P. Pouget and S. J. Mather, General aspects of the cellular response to low- and high-LET radiation. *Eur. J. Nucl. Med.* **28**, 541-561 (2001).

4.   C. J. Norbury and I. D. Hickson, Cellular responses to DNA damage. *Annu. Rev. Pharmacol. Toxicol.* **41**, 367-401 (2001).

5.   L. Galluzzi, M. C. Maiuri, I. Vitale, H. Zischka, M. Castedo, L. Zitvogel and G. Kroemer, Cell death modalities: classification and pathophysiological implications. *Cell Death Differ.* **14**, 1237-1243 (2007).

6.   W. C. Dewey, C. C. Ling and R. E. Meyn, Radiation-induced apoptosis: relevance to radiotherapy. *Int. J. Radiat. Oncol. Biol. Phys.* **33**, 781-796 (1995).

7.   R. Roots and S. Okada, Protection of DNA molecules of cultured mammalian cells from radiation-induced single-strand scissions by various alcohols and SH compounds. *Int. J. Radiat. Biol. Relat. Stud. Phys. Chem. Med.* **21**, 329-342 (1972).

8.   R. Hirayama, A. Ito, M. Tomita, T. Tsukada, F. Yatagai, M. Noguchi, Y. Matsumoto, Y. Kase, K. Ando, et al., Contributions of direct and indirect actions in cell killing by high-LET radiations. *Radiat. Res.* **171**, 212-218 (2009).

9.   D. T. Goodhead, Mechanisms for the biological effectiveness of high-LET radiations. *J. Radiat. Res. (Tokyo).* **40 Suppl**, 1-13 (1999).

10.   P. E. Bryant, Enzymatic restriction of mammalian cell DNA: evidence for double-strand breaks as potentially lethal lesions. *Int. J. Radiat. Biol. Relat. Stud. Phys. Chem. Med.* **48**, 55-60 (1985).

11.   S. Vispe and M. S. Satoh, DNA repair patch-mediated double strand DNA break formation in human cells. *J. Biol. Chem.* **275**, 27386-27392 (2000).

12.   M. Lobrich, P. K. Cooper and B. Rydberg, Non-random distribution of DNA double-strand breaks induced by particle irradiation. *Int. J. Radiat. Biol.* **70**, 493-503 (1996).

13. B. Stenerlow, E. Hoglund, K. Elmroth, K. H. Karlsson and I. Radulescu, Radiation quality dependence of DNA damage induction. *Radiat. Prot. Dosimetry* **99**, 137-141 (2002).

14. S. S. Wallace, Enzymatic processing of radiation-induced free radical damage in DNA. *Radiat. Res.* **150**, S60-79 (1998).

15. K. Magnander, R. Hultborn, K. Claesson and K. Elmroth, Clustered DNA damage in irradiated human diploid fibroblasts: influence of chromatin organization. *Radiat. Res.* **173**, 272-282 (2010).

16. M. Hada and B. M. Sutherland, Spectrum of complex DNA damages depends on the incident radiation. *Radiat. Res.* **165**, 223-230 (2006).

17. J. Nygren, M. Ljungman and G. Ahnstrom, Chromatin structure and radiation-induced DNA strand breaks in human cells: soluble scavengers and DNA-bound proteins offer a better protection against single- than double-strand breaks. *Int. J. Radiat. Biol.* **68**, 11-18 (1995).

18. C. Richardson and M. Jasin, Coupled homologous and nonhomologous repair of a double-strand break preserves genomic integrity in mammalian cells. *Mol. Cell Biol.* **20**, 9068-9075 (2000).

19. C. Allen, J. Halbrook and J. A. Nickoloff, Interactive competition between homologous recombination and non-homologous end joining. *Mol. Cancer Res.* **1**, 913-920 (2003).

20. K. Valerie and L. F. Povirk, Regulation and mechanisms of mammalian double-strand break repair. *Oncogene* **22**, 5792-5812 (2003).

21. B. K. Singleton, M. I. Torres-Arzayus, S. T. Rottinghaus, G. E. Taccioli and P. A. Jeggo, The C terminus of Ku80 activates the DNA-dependent protein kinase catalytic subunit. *Mol. Cell Biol.* **19**, 3267-3277 (1999).

22. Y. Ma, U. Pannicke, K. Schwarz and M. R. Lieber, Hairpin opening and overhang processing by an Artemis/DNA-dependent protein kinase complex in nonhomologous end joining and V(D)J recombination. *Cell* **108**, 781-794 (2002).

23. J. Huang and W. S. Dynan, Reconstitution of the mammalian DNA double-strand break end-joining reaction reveals a requirement for an Mre11/Rad50/NBS1-containing fraction. *Nucleic Acids Res.* **30**, 667-674 (2002).

24. H. L. Hsu, S. M. Yannone and D. J. Chen, Defining interactions between DNA-PK and ligase IV/XRCC4. *DNA Repair (Amst)* **1**, 225-235 (2002).

25. N. Saleh-Gohari and T. Helleday, Conservative homologous recombination preferentially repairs DNA double-strand breaks in the S phase of the cell cycle in human cells. *Nucleic Acids Res.* **32**, 3683-3688 (2004).

26. C. Wyman, D. Ristic and R. Kanaar, Homologous recombination-mediated double-strand break repair. *DNA Repair (Amst)* **3**, 827-833 (2004).

27. B. Stenerlow, E. Blomquist, E. Grusell, T. Hartman and J. Carlsson, Rejoining of DNA double-strand breaks induced by accelerated nitrogen ions. *Int. J. Radiat. Biol.* **70**, 413-420 (1996).

28. T. J. Jenner, C. M. deLara, P. O'Neill and D. L. Stevens, Induction and rejoining of DNA double-strand breaks in V79-4 mammalian cells following gamma- and alpha-irradiation. *Int. J. Radiat. Biol.* **64**, 265-273 (1993).

29. D. Blocher, DNA double-strand break repair determines the RBE of alpha-particles. *Int. J. Radiat. Biol.* **54**, 761-771 (1988).

30. M. A. Ritter, J. E. Cleaver and C. A. Tobias, High-LET radiations induce a large proportion of non-rejoining DNA breaks. *Nature* **266**, 653-655 (1977).

31. D. Klokov, S. M. MacPhail, J. P. Banath, J. P. Byrne and P. L. Olive, Phosphorylated histone H2AX in relation to cell survival in tumor cells and xenografts exposed to single and fractionated doses of X-rays. *Radiother. Oncol.* **80**, 223-229 (2006).

32. N. Foray, C. F. Arlett and E. P. Malaise, Radiation-induced DNA double-strand breaks and the radiosensitivity of human cells: a closer look. *Biochimie* **79**, 567-575 (1997).

33. B. Elliott and M. Jasin, Double-strand breaks and translocations in cancer. *Cell. Mol. Life Sci.* **59**, 373-385 (2002).

34. B. B. Zhou and S. J. Elledge, The DNA damage response: putting checkpoints in perspective. *Nature* **408**, 433-439 (2000).

35. J. Lukas, C. Lukas and J. Bartek, Mammalian cell cycle checkpoints: signalling pathways and their organization in space and time. *DNA Repair (Amst)* **3**, 997-1007 (2004).

36. J. H. Lee and T. T. Paull, Activation and regulation of ATM kinase activity in response to DNA double-strand breaks. *Oncogene* **26**, 7741-7748 (2007).

37. Y. Andegeko, L. Moyal, L. Mittelman, I. Tsarfaty, Y. Shiloh and G. Rotman, Nuclear retention of ATM at sites of DNA double strand breaks. *J. Biol. Chem.* **276**, 38224-38230 (2001).

38. J. Falck, N. Mailand, R. G. Syljuasen, J. Bartek and J. Lukas, The ATM-Chk2-Cdc25A checkpoint pathway guards against radioresistant DNA synthesis. *Nature* **410**, 842-847 (2001).

39. A. Hirao, Y. Y. Kong, S. Matsuoka, A. Wakeham, J. Ruland, H. Yoshida, D. Liu, S. J. Elledge and T. W. Mak, DNA damage-induced activation of p53 by the checkpoint kinase Chk2. *Science* **287**, 1824-1827 (2000).

40. S. Matsuoka, M. Huang and S. J. Elledge, Linkage of ATM to cell cycle regulation by the Chk2 protein kinase. *Science* **282**, 1893-1897 (1998).

41. T. Terasima and L. J. Tolmach, X-ray sensitivity and DNA synthesis in synchronous populations of HeLa cells. *Science* **140**, 490-492 (1963).

42. H. R. Withers, K. Mason, B. O. Reid, N. Dubravsky, H. T. Barkley, Jr., B. W. Brown and J. B. Smathers, Response of mouse intestine to neutrons and gamma rays in relation to dose fractionation and division cycle. *Cancer* **34**, 39-47 (1974).

43. R. P. Bird and H. J. Burki, Survival of synchronized Chinese hamster cells exposed to radiation of different linear-energy transfer. *Int. J. Radiat. Biol. Relat. Stud. Phys. Chem. Med.* **27**, 105-120 (1975).

44. F. Q. Ngo, E. A. Blakely, C. A. Tobias, P. Y. Chang and L. Lommel, Sequential exposures of mammalian cells to low- and high-LET radiations. II. As a function of cell-cycle stages. *Radiat. Res.* **115**, 54-69 (1988).

45. H. Wang, S. Liu, P. Zhang, S. Zhang, M. Naidu and Y. Wang, S-phase cells are more sensitive to high-linear energy transfer radiation. *Int. J. Radiat. Oncol. Biol. Phys.* **74**, 1236-1241 (2009).

46. F. Zafar, S. B. Seidler, A. Kronenberg, D. Schild and C. Wiese, Homologous recombination contributes to the repair of DNA double-strand breaks induced by high-energy iron ions. *Radiat. Res.* **173**, 27-39 (2010).

47. I. R. Radford, Effect of cell-cycle position and dose on the kinetics of DNA double-strand breakage repair in X-irradiated Chinese hamster cells. *Int. J. Radiat. Biol. Relat. Stud. Phys. Chem. Med.* **52**, 555-564 (1987).

48. K. Luger, A. W. Mader, R. K. Richmond, D. F. Sargent and T. J. Richmond, Crystal structure of the nucleosome core particle at 2.8 A resolution. *Nature* **389**, 251-260 (1997).

49. M. Falk, E. Lukasova and S. Kozubek, Chromatin structure influences the sensitivity of DNA to gamma-radiation. *Biochim. Biophys. Acta* **1783**, 2398-2414 (2008).

50. K. F. Toth, T. A. Knoch, M. Wachsmuth, M. Frank-Stohr, M. Stohr, C. P. Bacher, G. Muller and K. Rippe, Trichostatin A-induced histone acetylation causes decondensation of interphase chromatin. *J. Cell Sci.* **117**, 4277-4287 (2004).

51. K. B. Glaser, HDAC inhibitors: clinical update and mechanism-based potential. *Biochem. Pharmacol.* **74**, 659-671 (2007).

52. R. R. Rosato and S. Grant, Histone deacetylase inhibitors in clinical development. *Expert Opin. Investig. Drugs* **13**, 21-38 (2004).

53. I. Radulescu, K. Elmroth and B. Stenerlow, Chromatin organization contributes to non-randomly distributed double-strand breaks after exposure to high-LET radiation. *Radiat. Res.* **161**, 1-8 (2004).

54. C. P. Karger and O. Jakel, Current status and new developments in ion therapy. *Strahlenther. Onkol.* **183**, 295-300 (2007).

55. H. Song, R. F. Hobbs, R. Vajravelu, D. L. Huso, C. Esaias, C. Apostolidis, A. Morgenstern and G. Sgouros, Radioimmunotherapy of breast cancer metastases with alpha-particle emitter 225Ac: comparing efficacy with 213Bi and 90Y. *Cancer Res.* **69**, 8941-8948 (2009).

56. D. E. Milenic, K. J. Wong, K. E. Baidoo, T. K. Nayak, C. A. Regino, K. Garmestani and M. W. Brechbiel, Targeting HER2: a report on the in vitro and in vivo pre-clinical data supporting trastuzumab as a radioimmunoconjugate for clinical trials. *MAbs* **2**, 550-564 (2010).

57. G. W. Barendsen, C. J. Koot, G. R. Van Kersen, D. K. Bewley, S. B. Field and C. J. Parnell, The effect of oxygen on impairment of the proliferative capacity of human cells in culture by ionizing radiations of different LET. *Int. J. Radiat. Biol. Relat. Stud. Phys. Chem. Med.* **10**, 317-327 (1966).

58. H. Andersson, E. Cederkrantz, T. Back, C. Divgi, J. Elgqvist, J. Himmelman, G. Horvath, L. Jacobsson, H. Jensen, et al., Intraperitoneal alpha-particle radioimmunotherapy of ovarian cancer patients: pharmacokinetics and dosimetry of (211)At-MX35 F(ab')2--a phase I study. *J. Nucl. Med.* **50**, 1153-1160 (2009).

59. M. R. Zalutsky, D. A. Reardon, O. R. Pozzi, G. Vaidyanathan and D. D. Bigner, Targeted alpha-particle radiotherapy with 211At-labeled monoclonal antibodies. *Nucl. Med. Biol.* **34**, 779-785 (2007).

60. J. M. Burke, P. C. Caron, E. B. Papadopoulos, C. R. Divgi, G. Sgouros, K. S. Panageas, R. D. Finn, S. M. Larson, R. J. O'Reilly, et al., Cytoreduction with iodine-

131-anti-CD33 antibodies before bone marrow transplantation for advanced myeloid leukemias. *Bone Marrow Transplant.* **32**, 549-556 (2003).

61.   B. J. Allen, C. Raja, S. Rizvi, Y. Li, W. Tsui, P. Graham, J. F. Thompson, R. A. Reisfeld and J. Kearsley, Intralesional targeted alpha therapy for metastatic melanoma. *Cancer Biol. Ther.* **4**, 1318-1324 (2005).

62.   S. Nilsson, R. H. Larsen, S. D. Fossa, L. Balteskard, K. W. Borch, J. E. Westlin, G. Salberg and O. S. Bruland, First clinical experience with alpha-emitting radium-223 in the treatment of skeletal metastases. *Clin. Cancer Res.* **11**, 4451-4459 (2005).

63.   M. Lalande, A reversible arrest point in the late G1 phase of the mammalian cell cycle. *Exp. Cell Res.* **186**, 332-339 (1990).

64.   Y. Saintigny, F. Delacote, G. Vares, F. Petitot, S. Lambert, D. Averbeck and B. S. Lopez, Characterization of homologous recombination induced by replication inhibition in mammalian cells. *EMBO J.* **20**, 3861-3870 (2001).

65.   S. Lindegren, T. Back and H. J. Jensen, Dry-distillation of astatine-211 from irradiated bismuth targets: a time-saving procedure with high recovery yields. *Appl. Radiat. Isot.* **55**, 157-160 (2001).

66.   S. Palm, H. Andersson, T. Back, I. Claesson, U. Delle, R. Hultborn, L. Jacobsson, I. Kopf and S. Lindegren, In vitro effects of free 211At,211At-albumin and 211At-monoclonal antibody compared to external photon irradiation on two human cancer cell lines. *Anticancer Res.* **20**, 1005-1012 (2000).

67.   S. Lindegren, H. Andersson, T. Back, L. Jacobsson, B. Karlsson and G. Skarnemark, High-efficiency astatination of antibodies using N-iodosuccinimide as the oxidising agent in labelling of N-succinimidyl 3-(trimethylstannyl)benzoate. *Nucl. Med. Biol.* **28**, 33-39 (2001).

68.   S. Lindegren, S. Frost, T. Back, E. Haglund, J. Elgqvist and H. Jensen, Direct procedure for the production of 211At-labeled antibodies with an epsilon-lysyl-3-(trimethylstannyl)benzamide immunoconjugate. *J. Nucl. Med.* **49**, 1537-1545 (2008).

69.   N. Chouin, K. Bernardeau, F. Davodeau, M. Cherel, A. Faivre-Chauvet, M. Bourgeois, C. Apostolidis, A. Morgenstern, A. Lisbona and M. Bardies, Evidence of extranuclear cell sensitivity to alpha-particle radiation using a microdosimetric model. I. Presentation and validation of a microdosimetric model. *Radiat. Res.* **171**, 657-663 (2009).

70. B. M. Sutherland, P. V. Bennett, O. Sidorkina and J. Laval, Clustered damages and total lesions induced in DNA by ionizing radiation: oxidized bases and strand breaks. *Biochemistry (Mosc).* **39**, 8026-8031 (2000).

71. D. C. Schwartz and C. R. Cantor, Separation of yeast chromosome-sized DNAs by pulsed field gradient gel electrophoresis. *Cell* **37**, 67-75 (1984).

72. D. Blocher, In CHEF electrophoresis a linear induction of dsb corresponds to a nonlinear fraction of extracted DNA with dose. *Int. J. Radiat. Biol.* **57**, 7-12 (1990).

73. L. G. Littlefield, A. M. Sayer and E. L. Frome, Comparisons of dose-response parameters for radiation-induced acentric fragments and micronuclei observed in cytokinesis-arrested lymphocytes. *Mutagenesis* **4**, 265-270 (1989).

74. M. Fenech, W. P. Chang, M. Kirsch-Volders, N. Holland, S. Bonassi and E. Zeiger, HUMN project: detailed description of the scoring criteria for the cytokinesis-block micronucleus assay using isolated human lymphocyte cultures. *Mutat. Res.* **534**, 65-75 (2003).

75. E. Hoglund, E. Blomquist, J. Carlsson and B. Stenerlow, DNA damage induced by radiation of different linear energy transfer: initial fragmentation. *Int. J. Radiat. Biol.* **76**, 539-547 (2000).

76. H. C. Newman, K. M. Prise and B. D. Michael, The role of higher-order chromatin structure in the yield and distribution of DNA double-strand breaks in cells irradiated with X-rays or alpha-particles. *Int. J. Radiat. Biol.* **76**, 1085-1093 (2000).

77. B. Rydberg, Clusters of DNA damage induced by ionizing radiation: formation of short DNA fragments. II. Experimental detection. *Radiat. Res.* **145**, 200-209 (1996).

78. K. Elmroth and B. Stenerlow, Influence of chromatin structure on induction of double-strand breaks in mammalian cells irradiated with DNA-incorporated 125I. *Radiat. Res.* **168**, 175-182 (2007).

79. G. E. Iliakis, O. Cicilioni and L. Metzger, Measurement of DNA double-strand breaks in CHO cells at various stages of the cell cycle using pulsed field gel electrophoresis: calibration by means of 125I decay. *Int. J. Radiat. Biol.* **59**, 343-357 (1991).

80. B. M. Sutherland, P. V. Bennett, J. C. Sutherland and J. Laval, Clustered DNA damages induced by x rays in human cells. *Radiat. Res.* **157**, 611-616 (2002).

81. M. Gulston, J. Fulford, T. Jenner, C. de Lara and P. O'Neill, Clustered DNA damage induced by gamma radiation in human fibroblasts (HF19), hamster (V79-4) cells and plasmid DNA is revealed as Fpg and Nth sensitive sites. *Nucleic Acids Res.* **30**, 3464-3472 (2002).

82. D. Tsao, P. Kalogerinis, I. Tabrizi, M. Dingfelder, R. D. Stewart and A. G. Georgakilas, Induction and processing of oxidative clustered DNA lesions in 56Fe-ion-irradiated human monocytes. *Radiat. Res.* **168**, 87-97 (2007).

83. K. M. Prise, C. H. Pullar and B. D. Michael, A study of endonuclease III-sensitive sites in irradiated DNA: detection of alpha-particle-induced oxidative damage. *Carcinogenesis* **20**, 905-909 (1999).

84. A. Asaithamby, N. Uematsu, A. Chatterjee, M. D. Story, S. Burma and D. J. Chen, Repair of HZE-particle-induced DNA double-strand breaks in normal human fibroblasts. *Radiat. Res.* **169**, 437-446 (2008).

85. T. Groesser, H. Chang, G. Fontenay, J. Chen, S. V. Costes, M. Helen Barcellos-Hoff, B. Parvin and B. Rydberg, Persistence of gamma-H2AX and 53BP1 foci in proliferating and non-proliferating human mammary epithelial cells after exposure to gamma-rays or iron ions. *Int. J. Radiat. Biol.* (2011).

86. Z. Vilasova, M. Rezacova, J. Vavrova, A. Tichy, D. Vokurkova, F. Zoelzer, Z. Rehakova, J. Osterreicher and E. Lukasova, Changes in phosphorylation of histone H2A.X and p53 in response of peripheral blood lymphocytes to gamma irradiation. *Acta Biochim. Pol.* **55**, 381-390 (2008).

87. C. Mayer, O. Popanda, O. Zelezny, M. C. von Brevern, A. Bach, H. Bartsch and P. Schmezer, DNA repair capacity after gamma-irradiation and expression profiles of DNA repair genes in resting and proliferating human peripheral blood lymphocytes. *DNA Repair (Amst)* **1**, 237-250 (2002).

88. K. Hamasaki, K. Imai, K. Nakachi, N. Takahashi, Y. Kodama and Y. Kusunoki, Short-term culture and gammaH2AX flow cytometry determine differences in individual radiosensitivity in human peripheral T lymphocytes. *Environ. Mol. Mutagen.* **48**, 38-47 (2007).

89. H. Wang, X. Wang, P. Zhang and Y. Wang, The Ku-dependent non-homologous end-joining but not other repair pathway is inhibited by high linear energy transfer ionizing radiation. *DNA Repair (Amst)* **7**, 725-733 (2008).

90. C. Lucke-Huhle, E. A. Blakely, P. Y. Chang and C. A. Tobias, Drastic G2 arrest in mammalian cells after irradiation with heavy-ion beams. *Radiat. Res.* **79**, 97-112 (1979).

91. M. Scholz, W. Kraft-Weyrather, S. Ritter and G. Kraft, Cell cycle delays induced by heavy ion irradiation of synchronous mammalian cells. *Int. J. Radiat. Biol.* **66**, 59-75 (1994).

92.   S. T. Palayoor, J. L. Humm, R. W. Atcher, J. J. Hines and R. M. Macklis, G2M arrest and apoptosis in murine T lymphoma cells following exposure to 212Bi alpha particle irradiation. *Nucl. Med. Biol.* **20**, 795-805 (1993).

93.   M. R. Raju, T. S. Johnson, N. Tokita, S. Carpenter and J. H. Jett, Differences in cell-cycle progression delays after exposure to 238Pu alpha particles compared to X rays. *Radiat. Res.* **84**, 16-24 (1980).

94.   G. Buscemi, P. Perego, N. Carenini, M. Nakanishi, L. Chessa, J. Chen, K. Khanna and D. Delia, Activation of ATM and Chk2 kinases in relation to the amount of DNA strand breaks. *Oncogene* **23**, 7691-7700 (2004).

95.   E. Nasonova, K. Fussel, S. Berger, E. Gudowska-Nowak and S. Ritter, Cell cycle arrest and aberration yield in normal human fibroblasts. I. Effects of X-rays and 195 MeV u(-1) C ions. *Int. J. Radiat. Biol.* **80**, 621-634 (2004).

96.   S. Tenhumberg, E. Gudowska-Nowak, E. Nasonova and S. Ritter, Cell cycle arrest and aberration yield in normal human fibroblasts. II: Effects of 11 MeV u-1 C ions and 9.9 MeV u-1 Ni ions. *Int. J. Radiat. Biol.* **83**, 501-513 (2007).

97.   E. I. Azzam, S. M. de Toledo, A. J. Waker and J. B. Little, High and low fluences of alpha-particles induce a G1 checkpoint in human diploid fibroblasts. *Cancer Res.* **60**, 2623-2631 (2000).

98.   C. Lucke-Huhle, Alpha-irradiation-induced G2 delay: a period of cell recovery. *Radiat. Res.* **89**, 298-308 (1982).

99.   D. Deckbar, J. Birraux, A. Krempler, L. Tchouandong, A. Beucher, S. Walker, T. Stiff, P. Jeggo and M. Lobrich, Chromosome breakage after G2 checkpoint release. *J. Cell Biol.* **176**, 749-755 (2007).

100.   I. Diehl-Marshall and M. Bianchi, Induction of micronuclei by irradiation with neutrons produced from 600 MeV protons. *Br. J. Radiol.* **54**, 530-532 (1981).

101.   R. M. Anderson, S. J. Marsden, E. G. Wright, M. A. Kadhim, D. T. Goodhead and C. S. Griffin, Complex chromosome aberrations in peripheral blood lymphocytes as a potential biomarker of exposure to high-LET alpha-particles. *Int. J. Radiat. Biol.* **76**, 31-42 (2000).

102.   P. Virsik-Kopp and H. Hofman-Huether, Chromosome aberrations induced by high-LET carbon ions in radiosensitive and radioresistant tumour cells. *Cytogenet. Genome Res.* **104**, 221-226 (2004).

103. S. Paglin, T. Delohery, R. Erlandson and J. Yahalom, Radiation-induced micronuclei formation in human breast cancer cells: dependence on serum and cell cycle distribution. *Biochem. Biophys. Res. Commun.* **237**, 678-684 (1997).

104. A. Banasik, A. Lankoff, A. Piskulak, K. Adamowska, H. Lisowska and A. Wojcik, Aluminum-induced micronuclei and apoptosis in human peripheral-blood lymphocytes treated during different phases of the cell cycle. *Environ. Toxicol.* **20**, 402-406 (2005).

105. S. Masunaga, K. Ando, A. Uzawa, R. Hirayama, Y. Furusawa, S. Koike and K. Ono, The radiosensitivity of total and quiescent cell populations in solid tumors to 290 MeV/u carbon ion beam irradiation in vivo. *Acta Oncol.* **47**, 1087-1093 (2008).

106. S. Giunta, R. Belotserkovskaya and S. P. Jackson, DNA damage signaling in response to double-strand breaks during mitosis. *J. Cell Biol.* **190**, 197-207 (2010).

107. A. Krempler, D. Deckbar, P. A. Jeggo and M. Lobrich, An imperfect G2M checkpoint contributes to chromosome instability following irradiation of S and G2 phase cells. *Cell Cycle* **6**, 1682-1686 (2007).

108. J. Bussink, P. J. Tofilon and W. A. Brock, Repair of chromosome and DNA breaks versus cell survival in Chinese hamster cells. *Int. J. Radiat. Biol.* **70**, 23-32 (1996).

109. K. Rothkamm, I. Kruger, L. H. Thompson and M. Lobrich, Pathways of DNA double-strand break repair during the mammalian cell cycle. *Mol. Cell Biol.* **23**, 5706-5715 (2003).

110. I. A. Kim, J. H. Kim, J. H. Shin, I. H. Kim, J. S. Kim, H. G. Wu, E. K. Chie, Y. H. Kim, B. K. Kim, et al., A histone deacetylase inhibitor, trichostatin A, enhances radiosensitivity by abrogating G2/M arrest in human carcinoma cells. *Cancer Res. Treat.* **37**, 122-128 (2005).

111. F. Zhang, T. Zhang, Z. H. Teng, R. Zhang, J. B. Wang and Q. B. Mei, Sensitization to gamma-irradiation-induced cell cycle arrest and apoptosis by the histone deacetylase inhibitor trichostatin A in non-small cell lung cancer (NSCLC) cells. *Cancer Biol. Ther.* **8**, 823-831 (2009).

112. K. Elmroth, J. Nygren, L. J. Erkell and R. Hultborn, Radiation-induced double-strand breaks in mammalian DNA: influence of temperature and DMSO. *Int. J. Radiat. Biol.* **76**, 1501-1508 (2000).

113. K. Elmroth, J. Nygren, B. Stenerlow and R. Hultborn, Chromatin- and temperature-dependent modulation of radiation-induced double-strand breaks. *Int. J. Radiat. Biol.* **79**, 809-816 (2003).

114. H. C. Newman, K. M. Prise, M. Folkard and B. D. Michael, DNA double-strand break distributions in X-ray and alpha-particle irradiated V79 cells: evidence for non-random breakage. *Int. J. Radiat. Biol.* **71**, 347-363 (1997).

115. M. A. Walicka, G. Vaidyanathan, M. R. Zalutsky, S. J. Adelstein and A. I. Kassis, Survival and DNA damage in Chinese hamster V79 cells exposed to alpha particles emitted by DNA-incorporated astatine-211. *Radiat. Res.* **150**, 263-268 (1998).

116. C. Lucke-Huhle, W. Comper, L. Hieber and M. Pech, Comparative study of G2 delay and survival after 241 Americium-alpha and 60cobalt-gamma irradiation. *Radiat. Environ. Biophys.* **20**, 171-185 (1982).

117. Y. Yamada, Y. Oghiso, H. Enomoto and N. Ishigure, Induction of micronuclei in a rat alveolar epithelial cell line by alpha particle irradiation. *Radiat. Prot. Dosimetry* **99**, 219-222 (2002).

118. A. Bilbao, J. S. Prosser, A. A. Edwards, J. C. Moody and D. C. Lloyd, The induction of micronuclei in human lymphocytes by in vitro irradiation with alpha particles from plutonium-239. *Int. J. Radiat. Biol.* **56**, 287-292 (1989).

119. A. L. Brooks, G. J. Newton, L. J. Shyr, F. A. Seiler and B. R. Scott, The combined effects of alpha-particles and X-rays on cell killing and micronuclei induction in lung epithelial cells. *Int. J. Radiat. Biol.* **58**, 799-811 (1990).

120. E. Aurlien, R. H. Larsen, G. Akabani, D. R. Olsen, M. R. Zalutsky and O. S. Bruland, Exposure of human osteosarcoma and bone marrow cells to tumour-targeted alpha-particles and gamma-irradiation: analysis of cell survival and microdosimetry. *Int. J. Radiat. Biol.* **76**, 1129-1141 (2000).

121. T. Back, H. Andersson, C. R. Divgi, R. Hultborn, H. Jensen, S. Lindegren, S. Palm and L. Jacobsson, 211At radioimmunotherapy of subcutaneous human ovarian cancer xenografts: evaluation of relative biologic effectiveness of an alpha-emitter in vivo. *J. Nucl. Med.* **46**, 2061-2067 (2005).

122. J. Elgqvist, P. Bernhardt, R. Hultborn, H. Jensen, B. Karlsson, S. Lindegren, E. Warnhammar and L. Jacobsson, Myelotoxicity and RBE of 211At-conjugated monoclonal antibodies compared with 99mTc-conjugated monoclonal antibodies and 60Co irradiation in nude mice. *J. Nucl. Med.* **46**, 464-471 (2005).